

Measuring fractional charge and statistics in fractional quantum Hall fluids through noise experiments

Eun-Ah Kim,^{1,2} Michael J. Lawler,¹ Smitha Vishveshwara,¹ and Eduardo Fradkin¹

¹Department of Physics, University of Illinois at Urbana-Champaign, 1110 West Green Street, Urbana, Illinois 61801-3080, USA

²Stanford Institute for Theoretical Physics and Department of Physics, Stanford University, Stanford, California 94305, USA

(Received 13 April 2006; published 27 October 2006)

A central long standing prediction of the theory of fractional quantum Hall (FQH) states that it is a topological fluid whose elementary excitations are vortices with fractional charge and fractional statistics. Yet, the unambiguous experimental detection of this fundamental property, that the vortices have fractional statistics, has remained an open challenge. Here we propose a three-terminal “T junction” as an experimental setup for the direct and independent measurement of the fractional charge and statistics of fractional quantum Hall quasiparticles via cross current noise measurements. We present a nonequilibrium calculation of the quantum noise in the T-junction setup for FQH Jain states. We show that the cross current correlation (noise) can be written in a simple form, a sum of two terms, which reflects the braiding properties of the quasiparticles: the statistics dependence captured in a factor of $\cos \theta$ in one of two contributions. Through analyzing these two contributions for different parameter ranges that are experimentally relevant, we demonstrate that the noise at finite temperature reveals signatures of generalized exclusion principles, fractional exchange statistics and fractional charge. We also predict that the vortices of Laughlin states exhibit a “bunching” effect, while higher states in the Jain sequences exhibit an “antibunching” effect.

DOI: 10.1103/PhysRevB.74.155324

PACS number(s): 73.23.-b, 71.10.Pm, 73.50.Td, 73.43.Jn

I. INTRODUCTION

Bose-Einstein statistics of photons and Fermi-Dirac statistics of electrons hold keys to two major triumphs of quantum mechanics: the explanation of the blackbody radiation (that started quantum mechanics) and the periodic table. The spin-statistics theorem states that particles with integer (half-integer) spins are bosons (fermions) and that the corresponding second-quantized fields obey canonical equal time commutation (anticommutation) relations. In three spatial dimensions, the spin can only be integer or half-integer since the fields should transform as an irreducible representation of the Lorentz group SO(3, 1) (relativistic) or SO(3) (nonrelativistic). Consequently particles in three-dimensional (3D) space have either bosonic or fermionic statistics. In one spatial dimension (1D) on the other hand, neither fermions nor hardcore bosons can experience their statistics since they cannot go past each other. As a result, statistics is essentially arbitrary in one spatial dimension (which in some sense can even be regarded as a matter of definition.) In particular, the excitations of (integrable) one-dimensional systems are topological solitons which have a two-body S matrix which acquires a phase factor upon the exchange of the positions of the solitons. In this sense, one can assign an intermediate statistics to the solitons. However in two spatial dimensions the situation is quite different. It has long been known^{1,2} that in two dimensions an intermediate form of statistics, *fractional* statistics is possible. A specific quantum mechanical construction of a particle with fractional statistics, proposed and dubbed an *anyon* by Wilczek,² consists of a particle of charge q bound to a solenoid with flux ϕ , where $q\phi$ bears a noninteger ratio to the fundamental flux quantum ϕ_0 . In this paper, we study the 2D setting of the quantum Hall system as an arena for displaying such fractional statistics, and propose a concrete experiment for measuring its effects.

Not long after the first observation of the fractional quantum Hall (FQH) effect,³ Laughlin proposed that the quasipar-

ticles (QP's) and quasiholes (QH's) of these incompressible fluids carry a fractional charge $e^* = \pm ve$ determined by the precisely quantized Hall conductance $\nu = 1/(2n+1)$ for an integer n (for Laughlin states)⁴. Soon after, it was shown that these QP's, would have fractional braiding statistics,^{5,6} i.e., the two QP joint wave function would gain a complex valued phase factor interpolating between 1 (boson) and -1 (fermion) upon exchange:

$$\Psi(\mathbf{r}_1, \mathbf{r}_2) = e^{i\theta} \Psi(\mathbf{r}_2, \mathbf{r}_1) \quad (1.1)$$

with $0 < \theta < \pi$. In the anyonic picture, the statistical angle corresponds to $\theta = \pi q\phi/\phi_0$. Laughlin QP's are a specific example with $q = \nu$. In order to compute the statistical angle θ , Arovas *et al.*⁵ first considered the adiabatic process of one QP encircling another. By calculating the Berry phase associated with this process they showed that the two QP wave function $\Psi(\mathbf{r}_1, \mathbf{r}_2)$ gains an extra “statistical phase” of $e^{i2\nu\pi}$ in addition to the magnetic flux induced Aharonov-Bohm phase upon encircling. An adiabatic exchange of two QP's can be achieved by moving one QP only half its way around the other and shifting both of them rigidly to end up in interchanged initial positions. They thus argued that the phase factor picked up by a two QP joint wave function upon this exchange process should be precisely half of what it is for a round trip and hence $\theta = \nu\pi$.

From a more general standpoint, anyons are excitations which carry a representation of the braid group (see below). This is possible both for nonrelativistic particles in high magnetic fields (as we will be interested in here) as well as some field-theoretic relativistic models. As in the FQH example, the quantum mechanical amplitudes for processes involving two or more of these particles (regarded as low-energy excitations from some more complicated system) are represented by world lines which never cross (as if they had a hard-core repulsion). In (2+1) dimensions different histo-

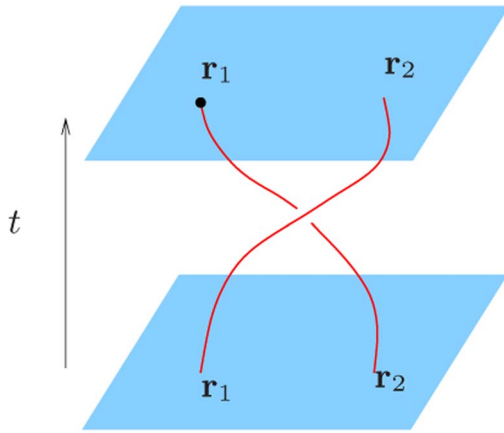


FIG. 1. (Color online) An adiabatic exchange between two QP's braids worlds lines representing histories of each QP.

ries of these particles can be classified according to the topological invariants of the knots formed by their world lines (see Fig. 1). These topological invariants are representations of a group, the braid group. The statistical angle is one such label and it corresponds to an Abelian (one-dimensional) representation of the braid group. Most quantum Hall states are Abelian (in this sense). However a number of non-Abelian states have been constructed (e.g., $\nu=5/2$, $12/5$, and a few others).

Fractional (or braid) statistics is a generalization of the concept that fermions have wave functions which are odd upon exchange (i.e., thus they obey the Pauli exclusion principle) while bosons have wave functions which are odd upon exchange. The notion of statistics is (as its name indicates) also related to the problem of counting states. Some years ago, Haldane⁷ introduced the concept of exclusion statistics, which is a generalization of the Pauli exclusion principle for fermions. Exclusion statistics in finite systems is determined by how much an addition of a particle diminishes the number of available states for yet another addition. For fermions, the number of states will diminish by 1 if a particle is added to the system while for bosons, the number of states would stay the same; Haldane's idea was to consider more general possibilities interpolating between fermions and bosons. Although the Hilbert space counting definition of statistics and the braiding definition of statistics coincide with one another for Laughlin states, the two definitions are not equivalent in general. It was argued by Haldane,⁷ and shown explicitly by Van Elburg and Schoutens,⁸ that the QP's of the FQH states also obey a form of exclusion statistics.

Fractional charge and statistics are fundamental properties of QP's emerging from the strongly interacting FQH liquid. Each of the filling factors ν displaying precise quantization of fractional Hall conductance $\sigma_{xy}=\nu e^2/h$ represent a distinct phase characterized by nontrivial internal order—topological order—which is robust against arbitrary perturbations.^{9,10} The measurement of fractional statistics will prove the existence of such topological order. While there is substantial experimental evidence for the fractional charge of these QP's and QH's,^{11–14} in particular from two-terminal noise experiments, similar evidence for statistical properties or the con-

TABLE I. Fractional charge e^* and statistical angle θ for QP's of FQH states at filling factor $\nu=p/(2np+1)$ (n , p are integers) in comparison with bosons and fermions following Ref. 17. Alternative descriptions predict somewhat different spectrum of QP's for non-Laughlin states at $p \neq 1$ (see Ref. 10) and implications of such differences will be discussed in the latter part of this paper.

	boson	$p=1$	$p>1$	fermion
e^*/e	$0, 2, \dots$	ν	$\frac{\nu}{p}$	1
θ/π	0	$\nu < \frac{1}{2}$	$(1 - \frac{2n}{p}\nu) > \frac{1}{2}$	1

nection between two distinct ways of determining statistics is still lacking. The main challenge in detection of anyons is to manipulate these “emergent particles” which cannot be taken outside the 2D system and to measure the effect of statistical phase. In this paper, we show that the noise in current fluctuations in a three-terminal geometry (a “T junction”) in FQH Jain states¹⁵ behaves as in a Hanbury-Brown and Twiss (HBT) interferometer¹⁶ with clear and independent signatures of fractional charge, fractional statistics and exclusion statistics.

Our interest in Jain states is twofold. First, the most prominent FQH effects which are observed lie in the Jain sequence with $\nu=\frac{p}{2np+1}$, where n and p are integers. Further, as shown in Table I, Jain states include “non-Laughlin states” with fractional charge and statistical angle that are different from the filling factor, i.e., $e^*/e \neq \theta/\pi \neq \nu$. Therefore one can pursue signatures of these fractional quantum numbers independently and predict how each fractional quantum numbers will manifest itself in different aspects of experimental data. Particularly, by comparing two FQH states whose QPS have same fractional charge but different statistics one can focus on the effects of fractional statistics.

In this paper we present a theory of noise cross correlations of the currents in a three-terminal junction (or T junction) which we introduced in Ref. 18, where we presented a summary of results of the theory. Here, we describe the theory and its conceptual and technical underpinnings in a more detailed and self-contained fashion. The bulk of the paper consists of the description of the cross current correlation between tunneling currents partitioned from one edge of the proposed T-junction setup into two others. The lowest order nonvanishing contribution to the correlation is fourth order in tunneling and it is the quantity that contains signatures of both fractional charge and fractional statistics. In particular, by analyzing the components of the correlation in depth, we pinpoint the role of statistics in various tunneling processes and discuss implications of the connection between braiding statistics and exclusion statistics.

The paper is organized as follows. In Sec. II we briefly review the effective theory for edge states developed in Ref. 17 which we will use throughout. In Sec. III, we introduce the T-junction setup we are proposing and we define the normalized cross current noise to be calculated perturbatively in Sec. IV. In Secs. V and VI, we present the time dependent noise and its frequency spectrum, respectively. We summarized our results and discuss its implications for experiments in Sec. VII. In four appendices we present a sum-

mary of the theory of the edge states that we use here (Appendix A), of the Schwinger-Keldysh technique and conventions (Appendix B), some useful identities for vertex operators (Appendix C), and the unitary Klein factors (Appendix D).

II. AN EFFECTIVE THEORY FOR EDGE STATES

In this section, we summarize the properties of edge states for the Jain sequence and their associated quasiparticles. While the creation of QP excitations in the 2D bulk of FQH systems has an associated energy gap (i.e., FQH liquid is incompressible), the one-dimensional (1D) boundary defined by a confining potential can support gapless excitations.^{10,19} Further there is a striking one-to-one correspondence between QP states in the bulk and at the edge making the FQH liquid holographic.¹⁹ Given that edge states comprise an effective 1D system propagating only along the direction dictated by the magnetic field (a chiral Luttinger liquid^{10,19}), they can be described in terms of chiral bosons using the standard bosonization approach. The edge effective Lagrangian density for Jain states, derived from the boundary term of the fermionic Chern-Simons theory²⁰ by López and Fradkin¹⁷ is given by

$$\begin{aligned} \mathcal{L}_0 = & \frac{1}{4\pi\nu} \partial_x \phi_c (-\partial_t \phi_c - \partial_x \phi_c) \\ & + \lim_{v_N \rightarrow 0^+} \frac{1}{4\pi} \partial_x \phi_N (\partial_t \phi_N + v_N \partial_x \phi_N), \end{aligned} \quad (2.1)$$

where ϕ_c is a right moving charge mode whose speed is set to be $v_c=1$ (ϕ_- with $g=1/\nu$ and $v=1$ case of Appendix A) and ϕ_N is the nonpropagating charge neutral topological mode obtained as a $v_N \rightarrow 0^+$ limit of a right mover with $g_N=-1$. Note that for the purpose of regularization and to carefully keep track of short time behavior which is crucial for ensuring the correct statistics, we shall keep a neutral mode speed v_N and take the limit $v_N \rightarrow 0$ only at the very end.

The normal ordered vertex operator creating a quasiparticle excitation on this edge, with fractional quantum numbers tabulated in Table I, is given by¹⁷

$$\psi^\dagger \propto :e^{-i[(1/p)\phi_c + \sqrt{1+(1/p)}\phi_N]}: \equiv :e^{-i\varphi}:, \quad (2.2)$$

where we define a short hand notation φ to represent the appropriate linear combination of the charge mode and the topological mode

$$\varphi \equiv \left(\frac{1}{p} \phi_c + \sqrt{1 + \frac{1}{p}} \phi_N \right). \quad (2.3)$$

By noting the equal time commutator for the new field φ being

$$\begin{aligned} [\varphi(x, t), \varphi(x', t)] &= i\pi \left(\frac{\nu}{p^2} - \frac{1}{p} - 1 \right) \text{sgn}(x - x') \\ &= -i\theta \text{sgn}(x - x') \end{aligned} \quad (2.4)$$

the quantum numbers of ψ^\dagger can be verified as follows. The charge density operator $j_0 \equiv \frac{1}{2\pi} \partial_x \phi_c$ measures the charge of

the QP operator since $[j_0(x), \psi^\dagger(x')] \equiv \frac{e^*}{e} \delta(x-x') \psi^\dagger(x')$. By expanding the vertex operator Eq. (2.2), this commutator can be calculated order by order to give

$$\begin{aligned} [j_0(x), \psi^\dagger(x')] &= \frac{1}{2\pi} [\partial_x \phi_c(x), e^{-i(1/p)\phi_c(x')}] \\ &= -\frac{1}{2\pi p} i \partial_x [\phi_c(x), \phi_c(x')] + \dots \\ &= \frac{1}{2\pi p} \partial_x \text{sgn}(x - x') + \dots \\ &= \frac{\nu}{p} \delta(x - x') \psi^\dagger(x'), \end{aligned} \quad (2.5)$$

hence $e^*/e = \frac{\nu}{p}$. As for statistics, using the Campbell-Baker-Hausdorff (CBH) formula for exponential of operators \hat{A} , $e^{\hat{A}} e^{\hat{B}} = e^{\hat{B}} e^{\hat{A}} e^{[\hat{A}, \hat{B}]}$, the statistical angle of the QP operator can be calculated via exchange of QP positions at equal time as the following:

$$\begin{aligned} \psi^\dagger(x) \psi^\dagger(x') &= \psi^\dagger(x') \psi^\dagger(x) e^{-[\varphi(x), \varphi(x')]} \\ &= \psi^\dagger(x') \psi^\dagger(x) e^{i\theta \text{sgn}(x-x')}, \end{aligned} \quad (2.6)$$

which confirms $\theta = (1 - \frac{2n}{p}\nu)$ modulo 2π .

Combining charge mode and neutral mode propagator, one can obtain the propagator for the field φ :

$$\begin{aligned} \langle \varphi(x, t) \varphi(0, 0) \rangle &= \frac{1}{p^2} \langle \phi_c(x, t) \phi_c(0, 0) \rangle + \left(1 + \frac{1}{p} \right) \\ &\quad \times \langle \phi_N(x, t) \phi_N(0, 0) \rangle \\ &= -\frac{\nu}{p^2} \ln \left[\frac{\tau_0 + i(t-x)}{\tau_0} \right] \\ &\quad + i \lim_{v_N \rightarrow 0^+} \frac{\pi}{2} \left(1 + \frac{1}{p} \right) \text{sgn}(v_N t - x). \end{aligned} \quad (2.7)$$

From Eq. (2.7), one arrives at the following form for the QP propagator at zero temperature (see Appendix C):

$$\begin{aligned} \langle \psi(x, t) \psi^\dagger(0, 0) \rangle &= e^{\langle \varphi(x, t) \varphi(0, 0) \rangle} \\ &= \lim_{v_N \rightarrow 0^+} \left[\frac{\tau_0}{\tau_0 + i(t-x)} \right]^{\nu/p^2} e^{-i(\pi/2)(1+1/p)\text{sgn}(v_N t - x)}. \end{aligned} \quad (2.8)$$

Equation (2.8) shows that the QP operators have the scaling dimension $\frac{K}{2} = \frac{\nu}{2p^2} = \frac{1}{2p(2np+1)}$. Further, as $\tau \rightarrow 0^+$, the limit $x \rightarrow 0^-$ of Eq. (2.8) becomes

$$\langle \psi(0^-, t) \psi^\dagger(0, 0) \rangle = \left| \frac{t}{\tau_0} \right|^{-K} e^{i\theta \text{sgn}(t)} \quad (2.9)$$

with the explicit dependence on the statistical angle emerging in the long wavelength limit. This equal position propagator, which explicitly encodes information on statistics, plays a prominent role in subsequent point-contact tunneling calculations. Most importantly, the amplitude of the propa-

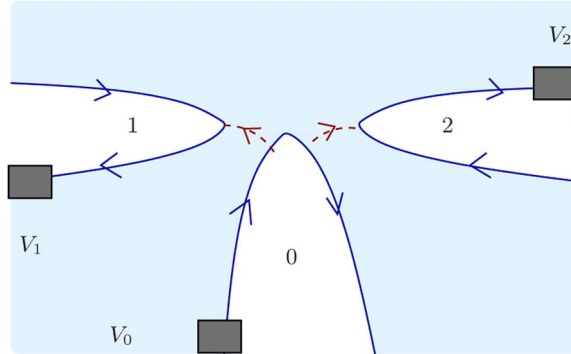


FIG. 2. (Color online) The proposed *T*-junction setup. Solid (blue) lines represent edge states where the edge state 0 is held at potential V relative to edges 1 and 2, i.e., $V_0 - V_1 = V_0 - V_2 = V$. Dashed (red) lines show paths of two quasiparticle tunneling through a FQH liquid from edge state 0 to edge 1 at $x_0 = -a/2 \equiv X_1$, $x_1 = 0$; from edge 0 to edge 2 at $x_0 = a/2 \equiv X_2$, $x_2 = 0$. The direct tunneling between edge 1 and 2 is turned off by setting the two edges at equal potential.

gator Eq. (2.9) is governed by the scaling dimension but the phase is solely determined by the statistical angle.

Since edge states are gapless excitations, they act as windows for experimental probes to observe features of the FQH droplet. In particular, tunneling between edges allows a viable access to single QP properties, provided the tunneling path lie inside the FQH liquid (QP's only exist within the liquid).²¹ In fact, such tunneling has been successfully used in a geometry hosting a single point contact and two edges for the detection of fractional charge through shot noise measurements.^{12–14} In principle, two edges would suffice for anyonic exchange as well with QP's from each edge exchanging positions via tunneling through the 2D FQH bulk. However, in order to detect the phase information, the path of exchange needs to be intercepted, for instance, by inserting a third edge and allowing QP exchange between first two edges to go through the third edge. This third edge thus acts at once as a stage and an “observation deck.” Further, if the first two edges are each adding/removing QP's to the third edge, one should be able to see the generalized exclusion principle in action by probing the third edge. In the next section, we propose a “*T*-junction” interferometer as a minimal realization of such a situation.

III. THE *T*-JUNCTION SETUP

In our proposed *T*-junction interferometer of the type shown in Fig. 2, top gates can be used to define and bring together three edge states $l=0,1,2$ which are separated from each other by ohmic contacts. Two edges $l=1$ and $l=2$ each separately form tunnel junctions with edge 0 and upon setting the edge 0 at relative voltage V to the two others, QP's are driven to tunnel between edge 0 and edges 1,2.

Denoting charge and neutral modes for edge $l=0,1,2$ by $\phi_c^l(x_l, t)$ and $\phi_N^l(x_l, t)$, respectively, each edge state l in the absence of tunneling (hence the superscript 0) can be described by Lagrangian densities of the form in Eq. (2.1):

$$\mathcal{L}_l^{(0)} = \frac{1}{4\pi\nu} \partial_{x_l} \phi_c^l (-\partial_t \phi_c^l - \partial_{x_l} \phi_c^l) + \frac{1}{4\pi} (\partial_{x_l} \phi_N^l \partial_t \phi_N^l), \quad (3.1)$$

where x_l now represents the curvilinear abscissa along each edge, and the total Lagrangian density becomes

$$\mathcal{L}^{(0)} = \sum_{l=0,1,2} \mathcal{L}_l^{(0)}. \quad (3.2)$$

Boson fields ϕ_c^l and ϕ_N^l each have the same properties (such as commutation relations and propagators) as ϕ_c and ϕ_N of a single edge described in the Sec. II. Fields of different edges commute with each other, i.e.,

$$[\phi_{c/N}^l, \phi_{c/N}^m] = 0, \quad \text{for } l \neq m \quad (3.3)$$

for $l, m = 0, 1, 2$. Within each edge l , a vertex operator $e^{i\varphi_l}$, where φ_l again is a short hand notation φ defined in Eq. (2.3) for each edge l , describes a QP excitation ψ_l^\dagger in that edge. However, since φ_l 's are constructed to commute between different edges, we need to introduce unitary Klein factors F_l with the appropriate algebra, as shown in the Appendix D, to give the correct QP statistics upon exchange between different edges. Hence, we have

$$\psi_l^\dagger = \frac{1}{\sqrt{2\pi a_0}} F_l e^{i[(1/p)\phi_c^l + \sqrt{1+(1/p)}\phi_N^l]} \equiv \frac{1}{\sqrt{2\pi a_0}} F_l e^{i\varphi_l}, \quad (3.4)$$

where a_0 is the short distance cutoff and the Klein factors obey the statistical rules

$$F_l F_m = e^{-i\alpha_{lm}} F_m F_l \quad (3.5)$$

where $\alpha_{lm} = -\alpha_{ml}$ and $\alpha_{02} = \alpha_{21} = -\alpha_{10} = \theta$. Notice the Klein factors do not affect the statistics between operators on the same edge since $\alpha_{ll} = 0$ from the requirement $\alpha_{lm} = -\alpha_{ml}$.

Now, if we set the the distance between two tunneling points on edge 0 to be a small positive real number a (which we later send to zero) and the tunneling point on edge 1, 2 to be the origin for the abscissa coordinate of edge 1, 2, then QP's tunnel at two locations $x_0 = -a/2 \equiv X_1$ and $x_0 = a/2 \equiv X_2$ on edge 0 and at $x_1 = 0, x_2 = 0$ on edges 1, 2. The operator $\hat{V}_j(t)$ which tunnels one QP from the edge 0 to edges $j = 1, 2$ at time t can then be written in the following form:

$$\hat{V}_j^\dagger(t) \equiv \psi_0(X_j, t) \psi_j^\dagger(0, t) = F_0 F_j^{-1} e^{i\varphi_0(X_j, t)} e^{-i\varphi_j(0, t)}. \quad (3.6)$$

The additional term in the Lagrangian due to the presence of the tunneling can be written as $L_{\text{int}} = L_{\text{int},1} + L_{\text{int},2}$ (Refs. 22 and 23) with tunneling term involving edges $j=1,2$ given by

$$L_{\text{int},j}(t) = -\Gamma_j \hat{V}_j^\dagger(t) + \text{H.c.}, \quad (3.7)$$

where Γ_j is the tunneling amplitude between edges 0 and $j = 1, 2$. The nonequilibrium situation of setting a constant dc voltage bias V between edges 0 and j corresponds to substituting Γ_j by $\Gamma_j e^{-i\omega_0 t}$ in Eq. (3.7), where the Josephson frequency is explicitly determined by the fractional charge to be $\omega_0 = e^* V / \hbar$ (the Peierls substitution^{22,24,25}). Using the Heisenberg equations of motion for the total charge $Q_l = \int dx_l j_{0l}(x_l)$ of edge l where $j_{0l}(x_l) = \frac{1}{2\pi} \partial_x \phi_c^l$ is the charge density operator for edge l , as was done by Chamon^{24,25} for

Laughlin states, one can show that the tunneling current operator $\hat{I}_j(t)$ from edge 0 to edge j is given by

$$\begin{aligned}\hat{I}_j(t) &= i \frac{e^*}{\hbar} \Gamma_j (e^{i\omega_0 t} \hat{V}_j^\dagger - e^{-i\omega_0 t} \hat{V}_j), \\ &\equiv ie^* \sum_{\epsilon=\pm} \epsilon \Gamma_j e^{i\epsilon\omega_0 t} \hat{V}_j^{(\epsilon)},\end{aligned}\quad (3.8)$$

where we assumed Γ_j to be real and introduced the notation $\hat{V}_j^\dagger \equiv \hat{V}_j^{(+)}$ and $\hat{V}_j \equiv \hat{V}_j^{(-)}$, i.e.,

$$\hat{V}_j^{(\epsilon)}(t) = (F_0 F_j^{-1})^\epsilon e^{i\epsilon\varphi_0(X_j,t)} e^{-i\epsilon\varphi_j(0,t)}, \quad (3.9)$$

to represent the summation over hermitian conjugates in a compact form. Notice that $\epsilon=+$ corresponds to a QP tunneling from the edge j to 0 and $\epsilon=-$ corresponds to a reverse direction tunneling.

We treat the nonequilibrium situation within the Schwinger-Keldysh formalism^{22–28} for computing expectation values of operators. As a simple example, the expectation value of the current on edge j takes the following form up to a normalization factor:

$$\langle I_j \rangle = \frac{1}{2} \sum_{\eta=\pm} \langle T_K \hat{I}_j(t^\eta) e^{i\int_K L_{\text{int},j}(t_j) dt_j} \rangle_0, \quad (3.10)$$

where η labels the branch of the Keldysh contour: $\eta=+$ for the forward branch ($t=-\infty \rightarrow \infty$) and $\eta=-$ for the backward branch ($t=\infty \rightarrow -\infty$). T_K indicates that the operators inside brackets should be contour ordered before taking the expectation value, and $\langle \cdot \rangle_0$ indicates the expectation value with respect to the free action $S_0 = \int_K dt \int d^3x \mathcal{L}_0$ where the free Lagrangian density \mathcal{L}_0 was given in Eq. (3.2).

Our goal is to identify a measurable quantity that distinctly captures the role of the statistical angle θ which features in the single QP operator shown in Eq. (2.6). The normalized cross correlation (noise) $S(t)$ between tunneling current fluctuations ($\Delta I_l = I_l - \langle I_l \rangle$):

$$S(t-t') \equiv \frac{\langle \Delta I_1(t) \Delta I_2(t') \rangle}{\langle I_1 \rangle \langle I_2 \rangle} \quad (3.11)$$

turns out to be the simplest quantity that can exhibit the subtle signatures of statistics and distinguish them from those of fractional charge. In fact, in contrast to shot noise, this cross current correlation $S(t-t')$ carries statistical information even at the lowest nontrivial order, which we calculate perturbatively in the next section.

IV. PERTURBATIVE CALCULATION

In this section, we perform a detailed analysis of the normalized cross correlation at fourth (lowest nonvanishing) order in tunneling. We calculate the two point correlation and four point correlation functions required to calculate the cross correlation in terms of edge state properties. We analyze the detailed behavior of the cross correlation over different Keldysh time domains and pinpoint the effects of statistics, specifically drawing the connection between braiding

statistics and exclusion statistics. We show that cross correlation can be expressed in terms of two universal scaling functions and that the statistical dependence ultimately takes on a remarkably simple form.

It must be remarked that since the perturbation introduced in Eq. (3.7) is relevant in the renormalization group sense, perturbation theory is valid only under certain conditions. Specifically, perturbation holds as long as energies involved, such as voltage and temperature, are higher than a crossover energy scale proportional to $\Gamma^{1/(1-K)}$. For energies much lower than this cross-over scale, QP tunneling between edges becomes large enough to break the Hall droplet into smaller disconnected regions and one needs an appropriate dual picture to properly address the strong coupling fixed point. For observing the effects of statistics as prescribed by the correlation calculated here, it is imperative that the system remains in the perturbative regime.

The unnormalized cross correlation $\langle I_1 \rangle \langle I_2 \rangle S(t-t')$ $= \langle \Delta I_1(t) \Delta I_2(t') \rangle$, where $\langle \cdot \cdot \cdot \rangle$ represents expectation value with respect to the full Lagrangian in the presence of tunneling events, can be written in terms of expectation values with respect to the free theory $\langle \cdot \rangle_0 \cdot \cdot \cdot$ as

$$\begin{aligned}\langle I_1 \rangle \langle I_2 \rangle S(t-t') &= \frac{1}{4} \sum_{\eta, \eta'} \langle T_K \hat{I}_1(t^\eta) \hat{I}_2(t'^{\eta'}) e^{i\int_K L_{\text{int},1}(t_1) dt_1 + i\int_K L_{\text{int},2}(t_2) dt_2} \rangle_0 \\ &\quad - \frac{1}{4} \sum_{\eta, \eta'} \langle T_K \hat{I}_1(t^\eta) e^{i\int_K L_{\text{int},1}(t_1) dt_1} \rangle_0 \times \\ &\quad \times T_K \hat{I}_2(t'^{\eta'}) e^{i\int_K L_{\text{int},2}(t_2) dt_2} \rangle_0.\end{aligned}\quad (4.1)$$

By expanding the exponentials in Eq. (4.1), we can calculate the cross correlation perturbatively in the tunneling amplitude Γ_j . Since the tunneling operator is relevant in the RG sense (its scaling dimension is less than 1), the perturbation theory will break down in the infrared (IR) limit. However, the finite temperature in our case provides a natural IR cutoff making this perturbative calculation meaningful. In fact, we will show in the following sections that the strongest statistical dependence is obtained at temperatures comparable to the bias voltage.

Clearly the lowest nonvanishing term in the perturbation expansion is of order $(\Gamma_1 \Gamma_2)^2$. Using the expression for the tunneling current operator in Eq. (3.8), the first term of Eq. (4.1) to this order can be written as

$$\begin{aligned}\langle I_1(t) I_2(t') \rangle^{(2)} &\equiv (-i)^2 (ie^*)^2 \frac{1}{4} \sum_{\eta, \eta', \eta_1, \eta_2} \sum_{\epsilon, \epsilon'} \epsilon \epsilon' \eta_1 \eta_2 |\Gamma_1 \Gamma_2|^2 \\ &\quad \times \int dt_1 dt_2 e^{i\epsilon \omega_0(t-t_1) + i\epsilon' \omega_0(t'-t_2)} \\ &\quad \times \langle T_K \hat{V}_1^{(\epsilon)}(t^\eta) \hat{V}_2^{(\epsilon')}(t'^{\eta'}) \hat{V}_1^{(-\epsilon)}(t_1^{\eta_1}) \hat{V}_2^{(-\epsilon')}(t_2^{\eta_2}) \rangle_0,\end{aligned}\quad (4.2)$$

where we used the fact that the Keldysh contour time-integral in the exponent can be represented using the contour branch index η'

$$\int_K dt = \sum_{\eta'=\pm} \eta' \int dt \quad (4.3)$$

and the charge neutrality condition discussed in Appendix C which enforces $\epsilon_1 = -\epsilon$ and $\epsilon_2 = -\epsilon'$. Similarly, the expectation value of the current for the second term of Eq. (4.1) becomes

$$\begin{aligned} \langle \hat{I}_1 \rangle^{(2)} &= \frac{1}{2} \sum_{\epsilon=\pm 1} \sum_{\eta, \eta_1} (-i)(ie^*)\epsilon \eta_1 \\ &\times \int dt_1 [|\Gamma_1|^2 e^{i\epsilon\omega_0(t-t_1)} \langle T_K \hat{V}_1^{(\epsilon)}(t^\eta) \hat{V}_1^{(-\epsilon)}(t_1^{\eta_1}) \rangle_0]. \end{aligned} \quad (4.4)$$

Putting Eqs. (4.2) and (4.4) together, we arrive at the following expression for the lowest nonvanishing term of the unnormalized cross current correlation

$$\begin{aligned} \langle I_1 \rangle \langle I_2 \rangle S^{(2)}(t-t') &= \frac{1}{4} (e^*)^2 \sum_{\eta, \eta', \eta_1, \eta_2} \sum_{\epsilon, \epsilon'} \epsilon \epsilon' \eta_1 \eta_2 |\Gamma_1 \Gamma_2|^2 \\ &\times \int dt_1 dt_2 e^{i\epsilon\omega_0(t-t_1) + i\epsilon'\omega_0(t'-t_2)} \\ &\times [\langle T_K \hat{V}_1^{(\epsilon)}(t^\eta) \hat{V}_2^{(\epsilon')}(t'^{\eta'}) \hat{V}_1^{(-\epsilon)}(t_1^{\eta_1}) \\ &\times \hat{V}_2^{(-\epsilon')}(t_2^{\eta_2}) \rangle_0 - \langle T_K \hat{V}_1^{(\epsilon)}(t^\eta) \hat{V}_1^{(-\epsilon)}(t_1^{\eta_1}) \rangle_0 \langle \\ &\times T_K \hat{V}_2^{(\epsilon')}(t'^{\eta'}) \hat{V}_2^{(-\epsilon')}(t_2^{\eta_2}) \rangle_0]. \end{aligned} \quad (4.5)$$

We now evaluate the two point function and the four point function, and then combine them to obtain a simplified formula for $\langle I_1 \rangle \langle I_2 \rangle S^{(2)}(t-t')$ from Eq. (4.5).

A. The two point function

Using Eq. (3.6) and the result of Appendix C to calculate the chiral boson vertex correlation function, we find

$$\begin{aligned} \langle T_K \hat{V}_1^{(\epsilon)}(t^\eta) \hat{V}_1^{(-\epsilon)}(t_1^{\eta_1}) \rangle_0 &= (F_0 F_1^{-1})^\epsilon (F_0 F_1^{-1})^{-\epsilon} \langle \\ &\times T_K e^{i\epsilon\varphi_0(X_1, t^\eta)} e^{-i\epsilon\varphi_0(X_1, t_1^{\eta_1})} \rangle \quad (4.6) \\ &= \exp[\tilde{G}_{\eta, \eta_1}(0, t-t_1)] \\ &\times \exp[\tilde{G}_{\eta, \eta_1}(0, t-t_1)], \end{aligned} \quad (4.7)$$

where $\tilde{G}_{\eta, \eta'}(x-x', t-t') \equiv \langle T_K \varphi_l(x, t^\eta) \varphi_l(x', t'^{\eta'}) \rangle_0$ is the Keldysh ordered and regulated φ_l propagator for all l which will be discussed below in detail for both zero temperature and finite temperatures. Here we also used the fact that φ_l 's are independent from each other for different l 's. Notice that the Klein factor contribution simply becomes an identity for a two point function of the tunneling operator \hat{V}_1 . Hence, Klein factors are not necessary in calculations involving two point functions alone, and in fact, this is the reason that the lowest order contribution to shot noise does not contain statistical information. However, as we show below, Klein factors have nontrivial contributions in the four point function which appears in the first term of Eq. (4.1).

We now focus on the form of $G_{\eta, \eta'}(-a, t-t')$ in the limit $a \rightarrow 0^+$. From the detailed analysis of Appendix B, the contour ordered propagators for ϕ_c and ϕ_N takes the following forms at finite temperatures:

$$\langle T_K \phi_c(x, t^\eta) \phi_c(x', t'^{\eta'}) \rangle = -\nu \ln \left[\frac{\sin \frac{\pi}{\beta} [\tau_0 + i\chi_{\eta, \eta'}(t-t') \{(t-t') - (x-x')\}]}{\frac{\pi\tau_0}{\beta}} \right] \quad (4.8)$$

$$\langle T_K \phi_N(x, t^\eta) \phi_N(x', t'^{\eta'}) \rangle = \lim_{v_N \rightarrow 0^+} -i \frac{\pi}{2} \chi_{\eta, \eta'} \operatorname{sgn}[v_N(t-t') - (x-x')]. \quad (4.9)$$

Hence the contour ordered propagator for φ represented by \tilde{G} in Eqs. (4.7) and (4.18) can be written as

$$\begin{aligned} \tilde{G}_{\eta, \eta'}(-a, t-t') &= -\frac{\nu}{p^2} \ln \left[\frac{\sin \frac{\pi}{\beta} [\tau_0 + i\chi_{\eta, \eta'}(t-t')(t-t'+a)]}{\frac{\pi\tau_0}{\beta}} \right] + \lim_{v_N \rightarrow 0^+} i \frac{\pi}{2} \left(\frac{1}{p} + 1 \right) \chi_{\eta, \eta'}(t-t') \operatorname{sgn}[v_N(t-t') + a]. \end{aligned} \quad (4.10)$$

For the case of interest, i.e., $a \rightarrow 0^+$ in the limit $\tau_0 \rightarrow 0^+$, the above takes the following form (see Appendix B):

$$\tilde{G}_{\eta,\eta'}(0^-, t-t') = \ln C(t-t'; T, K) + i\frac{\theta}{2} \chi_{\eta,\eta'}(t-t') \operatorname{sgn}(t-t'), \quad (4.11)$$

where we have introduced a notation for the amplitude of the QP propagator that depends on the temperature T and the scaling dimension $K=\nu/p^2$:

$$C(t; T, K) \equiv \frac{(\pi\tau_0)^K}{|\sinh \pi k_B T t|^K} \quad (4.12)$$

and defined

$$\chi_{\eta,\eta'}(t-t') \equiv \left(\frac{\eta+\eta'}{2} \operatorname{sgn}(t-t') - \frac{\eta-\eta'}{2} \right). \quad (4.13)$$

We can now calculate the expectation value of the tunneling current $\langle I_1 \rangle$ of Eq. (4.4) to order $O(\Gamma_1^2)$ using Eqs. (4.7) and (4.10),

$$\langle I_1(t^\eta) \rangle^{(2)} = e^* |\Gamma_1|^2 \sum_\epsilon \int dt_1 e^{i\epsilon\omega_0(t-t_1)} Y(\theta) C(t-t_1)^2 \quad (4.14)$$

with the statistical factor

$$Y(\theta) = \left(\sum_{\eta_1} \eta_1 e^{i\theta \chi_{\eta,\eta_1}(t-t_1) \operatorname{sgn}(t-t_1)} \right) = 2i \sin \theta. \quad (4.15)$$

Notice that the resulting $\langle I_1(t^\eta) \rangle$ is independent of η and is a constant independent of t , as applicable for a steady state current.

B. The four point function

Following a procedure similar to the one that led up to Eq. (4.7), we find that the four point function becomes

$$\begin{aligned} & \langle T_K \hat{V}_1^{(\epsilon)}(t^\eta) \hat{V}_2^{(\epsilon')}(t'^{\eta'}) \hat{V}_1^{(-\epsilon)}(t_1^{\eta_1}) \hat{V}_2^{(-\epsilon')}(t_2^{\eta_2}) \rangle_0 \\ &= \langle T_K e^{i\epsilon\varphi_0(X_1,t^\eta)} e^{i\epsilon'\varphi_0(X_2,t'^{\eta'})} e^{-i\epsilon\varphi_0(X_1,t_1^{\eta_1})} e^{-i\epsilon'\varphi_0(X_2,t_2^{\eta_2})} \rangle_0 \langle T_K e^{i\epsilon\varphi_1(0,t^\eta)} e^{-i\epsilon\varphi_1(0,t_1^{\eta_1})} \rangle_0 \langle \end{aligned} \quad (4.16)$$

$$\begin{aligned} & \times T_K e^{i\epsilon'\varphi_2(0,t'^{\eta'})} e^{-i\epsilon'\varphi_2(0,t_2^{\eta_2})} \rangle_0 \langle T_K (F_0 F_1^{-1})^\epsilon (F_0 F_2^{-1})^{\epsilon'} (F_0 F_1^{-1})^{-\epsilon} (F_0 F_2^{-1})^{-\epsilon'} \rangle_0 \\ &= e^{[\tilde{G}_{\eta,\eta_1}(0,t-t_1) + \tilde{G}_{\eta',\eta_2}(0,t'-t_2) + \epsilon\epsilon' \tilde{G}_{\eta,\eta_2}(-a,t-t_2) + \epsilon\epsilon' \tilde{G}_{\eta',\eta_1}(-a,t'-t_1) - \epsilon\epsilon' \tilde{G}_{\eta,\eta'}(a,t-t') - \epsilon\epsilon' \tilde{G}_{\eta_1,\eta_2}(-a,t_1-t_2)]} \\ & \times e^{\tilde{G}_{\eta,\eta_1}(0,t-t_1) \tilde{G}_{\eta',\eta_2}(0,t'-t_2)} \langle T_K (F_0 F_1^{-1})^\epsilon (F_0 F_2^{-1})^{\epsilon'} (F_0 F_1^{-1})^{-\epsilon} (F_0 F_2^{-1})^{-\epsilon'} \rangle_0 \end{aligned} \quad (4.17)$$

$$= e^{2[\tilde{G}_{\eta,\eta_1}(0,t-t_1) + \tilde{G}_{\eta',\eta_2}(0,t'-t_2)]} \frac{e^{\epsilon\epsilon'[\tilde{G}_{\eta,\eta_2}(-a,t-t_2) + \tilde{G}_{\eta',\eta_1}(a,t'-t_1)]}}{e^{\epsilon\epsilon'[\tilde{G}_{\eta,\eta'}(-a,t-t') + \tilde{G}_{\eta_1,\eta_2}(-a,t_1-t_2)]}} \langle T_K (F_0 F_1^{-1})^\epsilon (F_0 F_2^{-1})^{\epsilon'} (F_0 F_1^{-1})^{-\epsilon} (F_0 F_2^{-1})^{-\epsilon'} \rangle_0, \quad (4.18)$$

where we used Eq. (C6) for the case $N=4$ to calculate the four vertex correlator for the second equality and used the fact that $X_1-X_2=-a$.

The factor involving four sets of Klein factors of the form $(F_0 F_j^{-1})^\pm$ in the Eq. (4.18) has to be appropriately rearranged through proper exchange rules (D2) and (D5) as the tunneling operators $\hat{V}_j(t^\eta)$'s get rearranged for Keldysh contour ordering. Since contour ordering depends on time arguments of the tunneling operators, Klein factors effectively become endowed with dynamics in the sense that where each of these four times fall on the contour determines whether Klein factors associated with tunneling at each time have to be moved or not.²³ In order to rearrange four sets of combined Klein factors of the form $(F_0 F_j^{-1})^\epsilon(t^\eta)$ involved in Eq. (4.18), we have to take six different possible pairs and contour order within each pair. This process can be thought of as a full “contraction” where pairs of Klein factors can be treated akin to propagators.

These contour ordered Klein factor “propagators” were calculated in Appendix D to be

$$\begin{aligned} & \langle T_K (F_0 F_1^{-1})^\epsilon(t^\eta) (F_0 F_2^{-1})^{\epsilon'}(t'^{\eta'}) \rangle_0 = e^{i\epsilon\epsilon'(\theta/2)\operatorname{sgn}(X_1-X_2)\chi_{\eta,\eta'}(t-t')} \\ &= e^{-i\epsilon\epsilon'(\theta/2)\chi_{\eta,\eta'}(t-t')} \end{aligned} \quad (4.19)$$

$$\begin{aligned} & \langle T_K (F_0 F_2^{-1})^\epsilon(t^\eta) (F_0 F_1^{-1})^{\epsilon'}(t'^{\eta'}) \rangle_0 = e^{i\epsilon\epsilon'(\theta/2)\operatorname{sgn}(X_2-X_1)\chi_{\eta,\eta'}(t-t')} \\ &= e^{-i\epsilon\epsilon'(\theta/2)\chi_{\eta',\eta}(t'-t)}, \end{aligned} \quad (4.20)$$

where $\chi_{\eta,\eta'}(t)$ is defined in Eq. (4.13). Further using the fact that $F_0 F_j^{-1}$ commutes with itself gives

$$\langle T_K (F_0 F_j^{-1})^\epsilon(t^\eta) (F_0 F_j^{-1})^{-\epsilon'}(t'^{\eta'}) \rangle_0 = 1. \quad (4.21)$$

Expressing the Klein factor contribution in Eq. (4.18) in terms of the six possible pairs and using their forms given by Eqs. (4.20) and (4.21) simplifies it to the form

$$\frac{e^{-i\epsilon\epsilon'(\theta/2)\chi_{\eta,\eta_2}(t-t_2)}e^{-i\epsilon\epsilon'(\theta/2)\chi_{\eta_1,\eta'}(t_1-t')}}{e^{-i\epsilon\epsilon'(\theta/2)\chi_{\eta,\eta'}(t-t')}e^{-i\epsilon\epsilon'(\theta/2)\chi_{\eta_1,\eta_2}(t_1-t_2)}}. \quad (4.22)$$

Hence, we can rewrite the four point function of Eq. (4.18) as

$$\langle T_K \hat{V}_1^{(\epsilon)}(t^\eta) \hat{V}_2^{(\epsilon')}(t',\eta') \hat{V}_1^{(-\epsilon)}(t_1^{\eta_1}) \hat{V}_2^{(-\epsilon')}(t_2^{\eta_2}) \rangle_0 = e^{2[\tilde{G}_{\eta\eta_1}(0,t-t_1)+\tilde{G}_{\eta',\eta_2}(0,t'-t_2)]} \frac{e^{\epsilon\epsilon'[\tilde{G}_{\eta,\eta_2}(-a,t-t_2)-i(\theta/2)\chi_{\eta,\eta_2}(t-t_2)+\tilde{G}_{\eta_1,\eta'}(-a,t_1-t')-i(\theta/2)\chi_{\eta_1,\eta'}(t_1-t')]}}{e^{\epsilon\epsilon'[\tilde{G}_{\eta,\eta'}(-a,t-t')-i(\theta/2)\chi_{\eta,\eta'}(t-t')+\tilde{G}_{\eta_1,\eta_2}(-a,t_1-t_2)-i(\theta/2)\chi_{\eta_1,\eta_2}(t_1-t_2)]}}, \quad (4.23)$$

where we used the fact that $G_{\eta,\eta'}(x-x',t-t')=G_{\eta',\eta}(x'-x,t'-t)$, as is pointed out in Appendix B, to replace $G_{\eta',\eta_1}(a,t'-t_1)$ by $G_{\eta_1,\eta'}(-a,t_1-t')$.

Furthermore, observing the following:

$$\begin{aligned} & \tilde{G}_{\eta,\eta'}(0^-, t-t') - i\frac{\theta}{2}\chi_{\eta,\eta'}(t-t') \\ &= -K \ln \left| \frac{\sinh\left(\frac{\pi(t-t')}{\beta}\right)}{\frac{\pi\tau_0}{\beta}} \right| + i\frac{\theta}{2}\eta[1-\text{sgn}(t-t')] \end{aligned} \quad (4.24)$$

$$= \tilde{G}_{\eta,-\eta}(0^-, t-t'), \quad (4.25)$$

where we have used Eqs. (4.11) and (4.13), the four point function of Eq. (4.23) further simplifies to the final form

$$\begin{aligned} & \langle T_K \hat{V}_1^{(\epsilon)}(t^\eta) \hat{V}_2^{(\epsilon')}(t',\eta') \hat{V}_1^{(-\epsilon)}(t_1^{\eta_1}) \hat{V}_2^{(-\epsilon')}(t_2^{\eta_2}) \rangle_0 \\ &= e^{2[\tilde{G}_{\eta\eta_1}(0,t-t_1)+\tilde{G}_{\eta',\eta_2}(0,t'-t_2)]} \\ &\times \frac{e^{\epsilon\epsilon'[\tilde{G}_{\eta,-\eta}(0^-,t-t_2)+\tilde{G}_{\eta_1,-\eta_1}(0^-,t_1-t')]} }{e^{\epsilon\epsilon'[\tilde{G}_{\eta,-\eta}(0^-,t-t')+\tilde{G}_{\eta_1,-\eta_1}(0^-,t_1-t_2)]}} \end{aligned} \quad (4.26)$$

$$\begin{aligned} &= \left| \frac{(\pi\tau_0)^{2K}}{\sinh \frac{\pi(t-t_1)}{\beta}} \right|^{2K} \left| \frac{(\pi\tau_0)^{2K}}{\sinh \frac{\pi(t'-t_2)}{\beta}} \right|^{2K} \\ &\times \left| \frac{\sinh \frac{\pi(t_1-t_2)}{\beta}}{\sinh \frac{\pi(t_1-t')}{\beta}} \right|^{\tilde{\epsilon}K} \left| \frac{\sinh \frac{\pi(t-t')}{\beta}}{\sinh \frac{\pi(t-t_2)}{\beta}} \right|^{\tilde{\epsilon}K} \\ &\times e^{i\Phi_{\tilde{\epsilon}}^{\eta,\eta',\eta_1,\eta_2(t,t',t_1,t_2)}}, \end{aligned} \quad (4.27)$$

where we defined $\tilde{\epsilon}\equiv\epsilon\epsilon'$ noting that Eq. (4.23) depends only on the product $\epsilon\epsilon'$ and collected all contributions to the phase factor by defining the following function:

$$\begin{aligned} & \Phi_{\tilde{\epsilon}}^{\eta,\eta',\eta_1,\eta_2(t,t',t_1,t_2)} \\ &\equiv \theta\chi_{\eta,\eta_1}(t-t_1) + \theta\chi_{\eta',\eta_2}(t'-t_2) \\ &\quad - \tilde{\epsilon}\frac{\theta}{2}[\eta \text{sgn}(t-t_2) - \eta \text{sgn}(t-t')] \\ &\quad - \tilde{\epsilon}\frac{\theta}{2}[\eta_1 \text{sgn}(t_1-t') - \eta_1(t_1-t_2)] \quad (4.28) \\ &= -\eta\frac{\theta}{2}\{\text{sgn}(t-t_1) + \tilde{\epsilon} \text{sgn}(t-t_2) \\ &\quad - \tilde{\epsilon} \text{sgn}(t-t') - 1\} + \eta'\frac{\theta}{2} \\ &\quad \times \{1 - \text{sgn}(t'-t_2)\} - \eta_1\frac{\theta}{2} \\ &\quad \times \{-\text{sgn}(t-t_1) + \tilde{\epsilon} \text{sgn}(t_1-t')\} \\ &\quad - \tilde{\epsilon} \text{sgn}(t_1-t_2) - 1\} + \eta_2\frac{\theta}{2} \\ &\quad \times \{1 + \text{sgn}(t'-t_2)\}. \end{aligned} \quad (4.29)$$

Note that $\tilde{\epsilon}\equiv\epsilon\epsilon'$ depends only on the relative directions of tunneling, that is $\tilde{\epsilon}=+1$ for correlations between contributions to I_1 and I_2 in the same orientation ($\epsilon=\epsilon'$) and $\tilde{\epsilon}=-1$ for correlations between contributions to I_1 and I_2 in the opposite orientation ($\epsilon=-\epsilon'$). Each case of $\tilde{\epsilon}=\pm$ is illustrated in Fig. 3 labeled *S/O*, respectively. The fact that the phase factor Φ depends on these relative orientations allows us to understand the statistical angle dependent contribution to the noise in connection with exclusion statistics⁷ as we will discuss in the next section. Another important observation to be made in Eq. (4.29) is that the time dependence of the phase factor is such that it only depends on the sign of various time differences. Hence as we integrate over virtual times t_1 and t_2 , to evaluate $\langle I_1(t)I_2(0) \rangle$ according to Eq. (4.2), the domain of integration in (t_1, t_2) space can be divided into subdomains as shown in Fig. 4 and the phase factors for a given set of Keldysh branch indices η 's and relative orientation of tunneling $\tilde{\epsilon}$ may be computed. Since integration is additive, we can consider each domain's contribution separately and later add them up to unravel the effect of the phase factor. A simple analysis to follow shows that large parts of the (t_1, t_2)

space do not contribute to the integral due to vanishing summation over η 's. The remaining domains can then be assigned different values of overall constant from the summation over the phase factor.

C. The normalized noise

Putting Eq. (4.27) back into Eq. (4.2) for the $O(\Gamma_1^2 \Gamma_2^2)$ term of the current-current correlation and setting $t'=0$ (the expression has time translational invariance) and taking $t > 0$, we obtain for $\langle I_1(t)I_2(0) \rangle^{(2)}$

$$\begin{aligned} & \langle I_1(t)I_2(0) \rangle^{(2)} \\ &= (-i)^2 (ie^*)^2 \sum_{\eta_1, \eta_2} \sum_{\epsilon, \epsilon'} \epsilon \epsilon' \eta_1 \eta_2 |\Gamma_1 \Gamma_2|^2 \\ & \quad \times \int dt_1 dt_2 e^{i\epsilon \omega_0(t-t_1)-i\epsilon' \omega_0 t_2} e^{i\Phi_\epsilon^{\eta, \eta', \eta_1, \eta_2}(t, 0, t_1, t_2)} \\ & \quad \times \left(\frac{(\pi \tau_0)^{2K}}{\sinh \frac{\pi(t-t_1)}{\beta}} \right)^{2K} \left(\frac{(\pi \tau_0)^{2K}}{\sinh \frac{\pi t_2}{\beta}} \right)^{2K} \\ & \quad \times \left(\frac{\left| \sinh \frac{\pi(t_1-t_2)}{\beta} \right|^K}{\left| \sinh \frac{\pi t_1}{\beta} \right|^K} \right)^K \left(\frac{\left| \sinh \frac{\pi t}{\beta} \right|^K}{\left| \sinh \frac{\pi(t-t_2)}{\beta} \right|^K} \right)^K \epsilon \epsilon' \\ &= 2e^{*2} |\Gamma_1 \Gamma_2|^2 \sum_{\tilde{\epsilon}=\pm} \int dt_1 dt_2 \tilde{\epsilon} \cos[\omega_0(t-t_1-\tilde{\epsilon}t_2)] \\ & \quad \times \left(\sum_{\eta_1, \eta_2=\pm} \eta_1 \eta_2 e^{i\Phi_\epsilon^{\eta, \eta', \eta_1, \eta_2}(t, 0, t_1, t_2)} \right) \left(\frac{(\pi \tau_0)^{2K}}{\sinh \frac{\pi(t-t_1)}{\beta}} \right)^{2K} \\ & \quad \times \left(\frac{(\pi \tau_0)^{2K}}{\sinh \frac{\pi t_2}{\beta}} \right)^{2K} \\ & \quad \times \left(\frac{\left| \sinh \frac{\pi(t_1-t_2)}{\beta} \right|^K}{\left| \sinh \frac{\pi t_1}{\beta} \right|^K} \right)^K \left(\frac{\left| \sinh \frac{\pi t}{\beta} \right|^K}{\left| \sinh \frac{\pi(t-t_2)}{\beta} \right|^K} \right)^K \tilde{\epsilon}, \end{aligned} \quad (4.30)$$

where we separated the summation over Keldysh branch indices $\sum_{\eta, \eta', \eta_1, \eta_2}$ from the rest of the integrand using the fact that Keldysh branch index dependence enters the expression only through the total phase factor Φ . To get the second equality, we first used the identities $\sum_{\epsilon, \epsilon'=\pm} = \sum_{\epsilon, \tilde{\epsilon}=\pm}$ ($\tilde{\epsilon} \equiv \epsilon \epsilon'$) and then used $e^{i\epsilon \omega_0(t-t_1)-i\epsilon' \omega_0 t_2} = e^{i\epsilon \omega_0(t-t_1-\epsilon \epsilon' t_2)}$.

Now evaluating the summation over η 's:

$$\sum_{\eta_1, \eta_2=\pm} \eta_1 \eta_2 e^{i\Phi_\epsilon^{\eta, \eta', \eta_1, \eta_2}(t, 0, t_1, t_2)} \quad (4.31)$$

for different ranges of (t_1, t_2) , allows us to extract the statistical angle θ dependence of the cross correlation. To do so, we begin by noting that the expression for Φ Eq. (4.29) takes a constant value for different domains and hence the sum

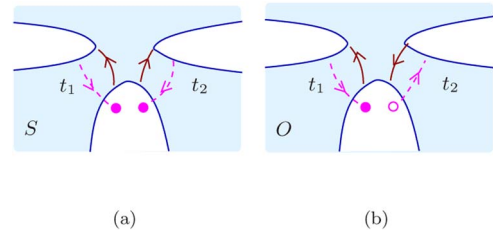


FIG. 3. (Color online) Virtual tunneling events taking place at all times t_1 and t_2 allowed by causality contribute to the noise (tunneling current cross-correlation) $S(t)$ in the lowest nonvanishing order. Solid (red) lines show paths of two quasiparticles tunneling through a FQH liquid from one edge state to two others (constituting I_1 and I_2) and dashed (magenta) lines represent virtual tunneling events. Depending on the relative orientation of the currents (or equivalently of the virtual processes) there are two cases: (a) the case S in which two currents are in the same orientation ($\tilde{\epsilon}=+1$ in the text) and (b) the case O in which two currents are in the opposite direction ($\tilde{\epsilon}=-1$ in the text).

over $\eta_1, \eta_2=\pm 1$ in the brackets of Eq. (4.30) can be independently evaluated prior to evaluating the integral if the virtual time (t_1, t_2) space is split into appropriate sub-domains. Consequently, we make the following observations.

(1) We first note that $\Phi_\epsilon^{\eta, \eta', \eta_1, \eta_2}(t, 0, t_1, t_2)$ is independent of η_2 for $t_2 > 0$. Since $\sum_{\eta_2=\pm 1} \eta_2 = 0$, the expression of Eq. (4.31) vanishes identically for $t_2 > 0$. Hence the only nonzero contribution to the integral comes from $t_2 < 0$.

(2) A similar consideration for the summation over η_1 for $t_1 > t$ allows us to limit the integration range to $t_1 < t$ since $\Phi_\epsilon^{\eta, \eta', \eta_1, \eta_2}(t, 0, t_1 > t, t_2 < 0)$ is independent of η_1 .

(3) The above analysis reflects the fact that only virtual times prior to the times of tunneling events can affect the correlation between tunneling events due to causality (thus acting as a check that our implementation of the Keldysh formalism for Klein factors is faithful in respecting causality).

(4) Now we are left only with the region $\{(t_1, t_2) | t_1 < t, t_2 < 0\}$ which is shaded in the Fig. 4. In this region, the phase of Eq. (4.29) simplifies to

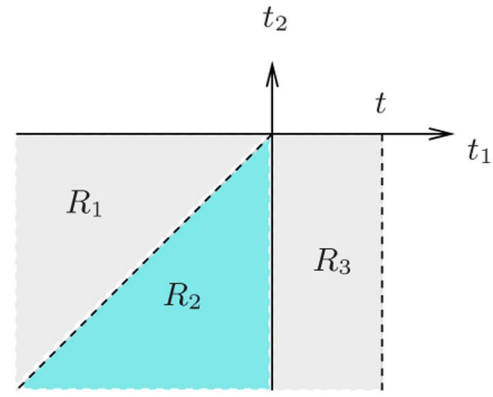


FIG. 4. (Color online) Subdomains of integration in the virtual time (t_1, t_2) space as it is defined in Eq. (4.34). Only the virtual times (t_1, t_2) that lie in the three shaded subdomains R_1 , R_2 , and R_3 give nonzero contribution to the cross current correlation (4.5) due to causality which is encoded in the Keldysh formalism.

$$\Phi_{\tilde{\epsilon}}^{\eta, \eta', \eta_1, \eta_2} = \theta \left[\eta_1 \left\{ 1 + \tilde{\epsilon} \left(\frac{\text{sgn}(t_1 - t_2) - \text{sgn}(t_1)}{2} \right) \right\} + \eta_2 \right], \quad (4.32)$$

where we used the fact that we are interested in the case $t > 0$. From this expression, which is independent of η and η' , we can identify three domains that contribute to the integral of Eq. (4.30):

$$\begin{aligned} R_1 &\equiv \{(t_1, t_2) | t_1 < t_2 < 0\}, \\ R_2 &\equiv \{(t_1, t_2) | t_2 < t_1 < 0\}, \\ R_3 &\equiv \{(t_1, t_2) | t_2 < 0 < t_1 < t\} \end{aligned} \quad (4.33)$$

as we depicted in Fig. 4.

(5) $\Phi_{\tilde{\epsilon}}^{\eta, \eta_1, \eta_2}(t, 0, t_1, t_2)$ can now be considered as a function that depends on the domain R_ζ ($\zeta=1, 2, 3$) which can be evaluated to give

$$\Phi_{\tilde{\epsilon}}^{\eta, \eta', \eta_1, \eta_2}[R_1] = \theta(\eta_1 + \eta_2), \quad (4.34)$$

$$\Phi_{\tilde{\epsilon}}^{\eta, \eta', \eta_1, \eta_2}[R_2] = \theta\{\eta_1(1 + \tilde{\epsilon}) + \eta_2\}, \quad (4.35)$$

$$\Phi_{\tilde{\epsilon}}^{\eta, \eta', \eta_1, \eta_2}[R_3] = \theta(\eta_1 + \eta_2). \quad (4.36)$$

It is worth noting that $\Phi_{\tilde{\epsilon}}$ has an explicit dependence upon $\tilde{\epsilon}$ only in the domain R_2 . However, since $\Phi_{\tilde{\epsilon}}^{\eta, \eta_1, \eta_2}[R_2]$ becomes independent of η_1 for $\tilde{\epsilon}=-1$, the sum (4.31) will once again vanish. Hence we find that only the case $\tilde{\epsilon}=+1$, where the calculated correlation is between the tunneling processes with same orientations (case *S* of Fig. 3), contributes to the part of the integral (4.30) coming from the domain R_2 . Later we will discuss the implication of this observation in more detail.

(6) Finally we can evaluate the phase factor summation over contour branch indices Eq. (4.31) for each regions using Eqs. (4.34)–(4.36) as the following:

$$\begin{aligned} \text{for } R_1: \sum_{\eta_1, \eta_2=\pm 1} \eta_1 \eta_2 e^{i\Phi_{\tilde{\epsilon}}^{\eta, \eta', \eta_1, \eta_2}[R_1]} \\ = \sum_{\eta_1, \eta_2=\pm 1} \eta_1 \eta_2 e^{i\theta(\eta_1 + \eta_2)} \\ = -4 \sin^2 \theta, \end{aligned} \quad (4.37)$$

$$\begin{aligned} \text{for } R_2: \sum_{\eta_1, \eta_2=\pm 1} \eta_1 \eta_2 e^{i\Phi_{\tilde{\epsilon}}^{\eta, \eta', \eta_1, \eta_2}[R_2]} \\ = \sum_{\eta_1, \eta_2=\pm 1} \eta_1 \eta_2 e^{i\theta(\eta_1(1 + \tilde{\epsilon}) + \eta_2)} \\ = \begin{cases} -4 \sin^2 \theta (2 \cos \theta) & \text{for } \tilde{\epsilon}=+1 \\ 0 & \text{for } \tilde{\epsilon}=-1 \end{cases}, \end{aligned} \quad (4.38)$$

$$\begin{aligned} \text{for } R_3: \sum_{\eta_1, \eta_2=\pm 1} \eta_1 \eta_2 e^{i\Phi_{\tilde{\epsilon}}^{\eta, \eta', \eta_1, \eta_2}[R_3]} \\ = \sum_{\eta_1, \eta_2=\pm 1} \eta_1 \eta_2 e^{i\theta(\eta_1 + \eta_2)} \\ = -4 \sin^2 \theta. \end{aligned} \quad (4.39)$$

At last, we can utilize the observations we made above to rewrite the four-point contribution to the noise $S(t)$ spelled out in Eq. (4.30) in the following form:

$$\begin{aligned} \langle I_1(t)I_2(0) \rangle^{(2)} &= -8 \sin^2 \theta e^{*2} |\Gamma_1 \Gamma_2|^2 \\ &\times \sum_{\tilde{\epsilon}=\pm} \int_{R_1, R_3} dt_1 dt_2 \tilde{\epsilon} \cos \omega_0(t - t_1 - \tilde{\epsilon} t_2) \\ &\times [C(t - t_1)C(t_2)]^2 \left[\frac{C(t_1)C(t - t_2)}{C(t_1 - t_2)C(t)} \right]^{\tilde{\epsilon}} \\ &- 16 \sin^2 \theta \cos \theta e^{*2} |\Gamma_1 \Gamma_2|^2 \int_{R_2} dt_1 dt_2 \cos \omega_0(t - t_1 - t_2) \\ &\times [C(t - t_1)C(t_2)]^2 \left[\frac{C(t_1)C(t - t_2)}{C(t_1 - t_2)C(t)} \right]. \end{aligned} \quad (4.40)$$

In Eq. (4.40) the statistical angle dependence has been extracted out and we found an additional factor of $2 \cos \theta$ in the contribution from the domain R_2 which does not occur in the contributions from domains R_1 and R_3 . We note that this contribution rises only from the case *S* of Fig. 3 (tunneling processes in the same orientation, i.e., $\tilde{\epsilon}=+1$) as is shown explicitly in the second equality of Eq. (4.40) by the value of $\tilde{\epsilon}$ being set to $+1$ in the contribution (the second term).

To complete our analysis, we now turn to the product of two point functions [the second term of Eq. (4.1)]. From Eq. (4.14), the second term of Eq. (4.1) to order $O(\Gamma_1^2 \Gamma_2^2)$ becomes

$$\begin{aligned} \langle I_1(t) \rangle \langle I_2(0) \rangle^{(2)} &= -4 \sin^2 \theta e^{*2} |\Gamma_1 \Gamma_2|^2 \sum_{\epsilon, \epsilon'=\pm} \epsilon \epsilon' \\ &\times \int dt_1 dt_2 e^{i\epsilon \omega_0(t-t_1) - i\epsilon' \omega_0(t_2)} C(t-t_1)^2 C(t_2)^2. \end{aligned} \quad (4.41)$$

Finally, putting all of the above together, the normalized noise (cross current correlation) is found to be of the following form:

$$\begin{aligned} S(\tilde{t}; T/T_0, K) &= \sum_{\zeta=1, 3} \sum_{\tilde{\epsilon}=\pm} S_{\zeta}^{\tilde{\epsilon}}(\tilde{t}; T/T_0, K) - 1 \\ &+ 2 \cos \theta S_2^+(\tilde{t}; T/T_0, K), \end{aligned} \quad (4.42)$$

where $S_{\zeta}^{\tilde{\epsilon}}(t)$ for all values of $\tilde{\epsilon}=\pm$ and $\zeta=1, 2, 3$ is defined by an integral over domain R_ζ for contributions with relative orientation of tunneling $\tilde{\epsilon}$ normalized by the product of the average tunneling current

$$S_{\zeta}^{\tilde{\epsilon}}(\tilde{t}; T/T_0, K) \equiv \frac{\tilde{\epsilon} \int_{R_{\zeta}} d\tilde{t}_1 d\tilde{t}_2 \cos(\tilde{t} - \tilde{t}_1 - \tilde{\epsilon} \tilde{t}_2) (C(\tilde{t} - \tilde{t}_1) C(\tilde{t}_2))^2 \left[\frac{C(\tilde{t}_1) C(\tilde{t} - \tilde{t}_2)}{C(\tilde{t}_1 - \tilde{t}_2) C(\tilde{t})} \right]^{\tilde{\epsilon}}}{\sum_{\tilde{\epsilon}' = \pm 1} \sum_{\zeta' = 1, 2, 3} \int_{R_{\zeta'}} d\tilde{t}_1 d\tilde{t}_2 \cos[\tilde{t} - \tilde{t}_1 - \tilde{\epsilon}' \tilde{t}_2] C(\tilde{t} - \tilde{t}_1)^2 C(\tilde{t}_2)^2}, \quad (4.43)$$

where we defined the dimensionless time $\tilde{t} \equiv \omega_0 t$ and also introduced a notation for the temperature equivalent to the Josephson frequency to be $T_0 \equiv \hbar \omega_0 / k_B$ and used the fact that $C(t; T, K) = C(\tilde{t}; T/T_0, K)$ from Eq. (4.12). Note that since we chose to study the normalized noise, all cutoff dependence and tunneling amplitude dependence in the noise is eliminated through normalization since they enter as common factors for numerator and denominator of Eq. (4.43).

D. Discussion

Now we can define two scaling functions \mathcal{A} and \mathcal{B} that depend on the scaling dimension K , the Josephson frequency $\omega_0 = e^* V / \hbar$ (or T_0) and the temperature as

$$\mathcal{A}(\omega_0 t; T/T_0, K) \equiv \sum_{\zeta=1,3} \sum_{\tilde{\epsilon}=\pm} S_{\zeta}^{\tilde{\epsilon}}(\omega_0 t; T/T_0, K) - 1, \quad (4.44)$$

$$\mathcal{B}(\tilde{t}; T/T_0, K) \equiv 2S_2^+(\omega_0 t; T/T_0, K). \quad (4.44)$$

We can thus rewrite Eq. (4.42) as a sum of two scaling functions, corresponding to a “direct term” and an “exchange term” which depends explicitly on $\cos \theta$:

$$S\left(\omega_0 t; \frac{T}{T_0}, K\right) = \mathcal{A}\left(\omega_0 t; \frac{T}{T_0}, K\right) + \cos \theta \mathcal{B}\left(\omega_0 t; \frac{T}{T_0}, K\right), \quad (4.45)$$

where $T_0 = \hbar \omega_0 / k_B$. Hence we were able to extract the statistical angle dependence of the noise in the form of the factor of $\cos \theta$ in the second term while both of the scaling functions \mathcal{A} and \mathcal{B} do not depend on the statistics. Equation (4.45) is the key result of this paper. One can gain further insight by recognizing the fact that the domain R_1 (which contributes to \mathcal{A}) and R_2 (which contributes to \mathcal{B}) are related to each other via exchange of virtual times t_1 and t_2 (see Fig. 4). In the following we discuss the physics behind the factor $\cos \theta$ in Eq. (4.45) with an eye towards bridging the connection between exclusion statistics and exchange statistics in our setup.

This expression displays a number of noteworthy properties.

- (a) This finite temperature result is applicable to all Jain states (in contrast to recent zero temperature results on Laughlin states^{22,29}) and it is a universal scaling function to the lowest order in perturbation theory which is valid provided the tunneling current is small compared to the Hall current.
- (b) Fractional charge and statistics play fundamentally distinct roles, each entering Eq. (4.45) through different features:

fractional charge through $\omega_0 = e^* V / \hbar$ and fractional statistics through the $\cos \theta$ factor.

(c) Given that for Laughlin states $\theta < \pi/2$ and $\cos \theta > 0$, the exchange term in Eq. (4.45) provides largely positive (“bunching,” bosonlike) contributions to the noise whereas for non-Laughlin states with $\theta > \pi/2$, its contribution is largely negative (“antibunching,” fermionlike).

(d) The fact that only case S, of Fig. 2, contributes to this factor can be viewed as a manifestation of a generalized exclusion principle⁷ since the virtual processes in this case involves adding a QP to edge 0 in the presence of another. It is noteworthy that we arrived at an observable consequence of a generalized exclusion principle given that Eq. (4.45) was derived using anyonic commutation rules prescribed by braiding statistics.⁵

A few remarks are in order here. For the function in Eq. (4.45) to be observable, given that it is the ratio between the cross-current correlations and the average values of the currents involved, the former needs to be at least comparable to the latter. As mentioned above, the form of the function only takes into account the lowest order terms in tunneling; when higher order terms become important, the function no longer remains universal in that it exhibits an explicit dependence on tunneling amplitudes. We assumed that tunneling from edge 0 occurred from a single point. In our calculations, we could have in principle retained the separation scale “ a ” for points from which QP’s tunnel into edges 1 and 2, respectively. Then, $1/a$ would enter the problem as another energy scale. The scaling function would depend on another parameter $\omega_0 a$ and the cross-current correlations would decay with separation length.

As one might expect from the simple form of the statistical angle dependence of Eq. (4.45), this expression can be understood in terms of simple pictures in which the setup simultaneously acts as an accessible stage for exchange processes and a testbed for generalized exclusion. To see that the form of Eq. (4.45) derives directly from exchange of QP’s between edges 1 and 2 via edge 0, we first note that information regarding anyonic exchange statistics and related time ordering of events is carried as a phase factor in the QP propagators. Contour ordering of events and associated time-dependent shuffling is completely contained in this exchange statistics phase factor. The following analysis of tunneling events and their effect on the phase factor not only shows that the simple $\cos \theta$ factor in Eq. (4.45) naturally emerges from the events associated with exchange statistics, but that it is also a manifestation of exclusion statistics.

Given that causality constrains lowest order virtual processes to occur at times t_1 and t_2 within domains R_1 , R_2 , and R_3 of Fig. 4, a QP/QP from edge 1 cannot exchange with a

QP/QH from edge 2 when $t_1 > 0$ (domain R_3) since QP/QH tunnels between edge 2 and edge 0 via virtual process at time $t_2 < 0$ and back at time 0 before anything happens between 1 and 0. Hence it is clear as to why $S_3^{\tilde{\epsilon}}$ coming from domain R_3 contributes to \mathcal{A} and an uncorrelated two-point piece is subtracted out.

Now for domains R_1 and R_2 , there is an overlap $|t_1 - t_2|$ in the times during which QP/QH's from edge 1 and edge 2 stay in edge 0 and hence can experience statistics induced interference. Between R_1 and R_2 , the only pairs of time whose relative orders change from one domain to the other is t_1 and t_2 and hence R_1 and R_2 are related to each other via exchange of entities involved in the virtual processes occurring at t_1 and t_2 . For both domains, depending on the relative orientations of the currents, the virtual tunneling processes leave two distinct pairs of objects at edge 0 as shown in Fig. 3.

In case S ($\tilde{\epsilon} = +1$), where I_1 and I_2 have the same orientation, the entities left behind are a pair of QP's. Hence the domain R_2 is related to the domain R_1 via exchange of these two identical particles. This exchange between two QP's brings in an additional phase factor of $e^{i\eta_1\theta}$ in Eq. (4.38) for the case $\tilde{\epsilon} = +$ that adds (constructive interference) to the phase factor $e^{i\eta_1\theta+i\eta_2\theta}$ that is common to all three domains [see Eqs. (4.37)–(4.39)] and also to the uncorrelated piece. Since the $\tilde{\epsilon}$ independent phase factor sum for domains R_1 , $-4 \sin^2 \theta$, is the same as that of the uncorrelated piece that normalizes the noise (and that for the domain R_3), it cancels upon normalization while the phase factor sum from the case S of domain R_2 results in the factor of $2 \cos \theta = \sin 2\theta / \sin \theta$. As a consequence $S_1^{\tilde{\epsilon}}$ is a part of \mathcal{A} without statistical angle dependence while S_2^+ enters \mathcal{B} . In case O ($\tilde{\epsilon} = -1$), on the other hand, tunneling currents have opposite orientations leaving one QP and one QH behind. Exchange between QP and QH brings in an additional phase of $e^{-i\eta_1\theta}$ in R_2 [see Eq. (4.38) for $\tilde{\epsilon} = -$] that cancels with the common phase factor $e^{i\eta_1\theta}$ (destructive interference) resulting in $\sin(\theta - \theta) = 0$ for the phase factor sum. Hence there is no S_2^- contribution to \mathcal{B} but only S_2^+ constitutes \mathcal{B} .

The generalized exclusion statistics is defined by counting the change in the one particle Hilbert space dimensions d_α for particles of species α as particles are added (keeping the boundary conditions and the size of the system constant) in the presence of other particles.^{7,8} The defining quantity for this description of fractional statistics is the statistical interaction $g_{\alpha\beta}$

$$\Delta d_\alpha = - \sum_\beta g_{\alpha\beta} \Delta N_\beta, \quad (4.46)$$

where $\{\Delta N_\beta\}$ is a set of allowed changes of the particle numbers at fixed size and boundary conditions boundary conditions. For bosons (without hardcore) $g_{\alpha\beta} = 0$, while the Pauli exclusion principle for fermions correspond to $g_{\alpha\beta} = \delta_{\alpha\beta}$. Thus, while the presence of bosons does not change the available number of states for an additional boson, the presence of a fermion reduces the number of available states by one. Once one understands the one particle Hilbert space of the particle of interest, the statistical interaction $g_{\alpha\beta}$ can be

calculated through state counting and for FQH QP's such program can be carried out using conformal field theory (CFT) as shown by van Elburg and Schoutens.⁸

However, the connection between this definition and an experimentally measurable quantity has not been clear so far. Further, the connection between fractional statistics defined through exclusion and anyonic statistics defined through exchange has not been clearly established for the following reason. The anyonic exchange for FQH QP's based on braid groups defined in Refs. 1 and 2 is achieved through attaching Chern-Simons flux to hardcore bosons³⁰ or spinless fermions.²⁰ However, how such flux attachments would affect Hilbert space dimensions is not obvious. For Laughlin QP's, one can use the knowledge of the chiral Hilbert space from CFT (Ref. 8) to find that the two definitions coincide. Nonetheless, an equivalent understanding for non-Laughlin states are still lacking.

In our setup, it is quite clear that only virtual processes occurring in domains R_1 and R_2 with $\tilde{\epsilon} = +1$ (case S in Fig. 3) host the situation of a QP being added in the presence of the other. The difference between R_1 and R_2 is the following: In R_1 , a QP from edge 2 tunnels in to edge 0 at time t_2 and leaves at time 0 with the QP from edge 1 present throughout. In R_2 , however, a QP from edge 1 tunnels in to the edge 0 at time t_1 later “pushing” a QP to edge 2 at time t_2 . Therefore virtual processes occurring in domain R_2 should be affected by statistical interaction of the generalized exclusion principle and we can understand why S_2^+ alone consists the statistics dependent term from this simple reasoning.

It is astonishingly consistent that the processes contributing to noise in which the generalized exclusion principle should manifest itself are the ones that are associated with the simple factor $\cos \theta$ considering that the statistical angle is what defines exchange (braiding) statistics. The fact that our results describe an experimentally measurable quantity makes it even more interesting. Although the manner in which the factor can be related to $g_{\alpha\beta}$ defined in Eq. (4.46) needs further investigation, it is clear from our choice of setup which allows access to the phase gain upon exchange while satisfying conditions for observation of generalized exclusion principle, that the connection exists. In the following sections, we analyze the scaling functions $\mathcal{A}(t)$ and $\mathcal{B}(t)$ after carrying out the integration over respective domains numerically and show that the noise experiment of the type proposed here can be used to detect and measure fractional statistics.

V. THE TIME DEPENDENT NOISE $S(t)$ ANALYSIS

Since the definite double integral in the numerator of the expression for $S_\zeta^{\tilde{\epsilon}}$ Eq. (4.43) does not grant an analytic expression in closed form, we evaluate $S_\zeta^{\tilde{\epsilon}}$ numerically. The integrable singularity in the vicinity of the domain boundary is regulated through a short time cutoff τ_0 . A natural choice for this cutoff that is intrinsic to QH system would be the inverse cyclotron frequency ω_c^{-1} , with $\omega_c \hbar \sim 1$ meV for the magnetic field of order 10 T required for the FQH. As we will discuss later, given that ω_c is such a high energy scale when compared to other important energy scales of the setup,

namely the Josephson frequency $\omega_0\hbar \equiv e^*V$ and the temperature $k_B T$, as ought to be the case, all interesting features of the noise turn out to be cutoff independent.

Before we discuss the results of our numerical integration, we can gain some insight by looking into the asymptotic behavior of $S_{\zeta}^{\tilde{\epsilon}}(\omega_0 t)$ in the short time limit $k_B T t, \omega_0 t \ll 1$ and in the long time limit $k_B T t, \omega_0 t \gg 1$. In the short time limit, the numerator of Eq. (4.43) becomes

$$\begin{aligned} S_{\zeta}^{\tilde{\epsilon}}(t) &\propto \tilde{\epsilon} |k_B T t|^{\tilde{\epsilon} K} \int_{R_{\zeta}} d\tilde{t}_1 d\tilde{t}_2 \cos(\tilde{t}_1 + \tilde{\epsilon} \tilde{t}_2) \\ &\times [C(\tilde{t}_1) C(\tilde{t}_2)]^2 \left| \frac{C(\tilde{t}_1) C(\tilde{t}_2)}{C(\tilde{t}_1 - \tilde{t}_2)} \right|^{\tilde{\epsilon}}, \end{aligned} \quad (5.1)$$

where we used

$$\lim_{t \rightarrow 0} C(t) \propto |\pi k_B T t|^{-K}. \quad (5.2)$$

Since the domain size of R_3 is proportional to t , the integral in Eq. (5.1) is negligible for $\zeta=3$ and hence we can ignore $S_3^{\tilde{\epsilon}}$'s contribution to \mathcal{A} as $t \rightarrow 0$. However since the integral in Eq. (5.1) is independent of t for domains R_1 and R_2 , $S_1^+(t)$ diverges as $(k_B T t)^{-K}$ for $\tilde{\epsilon}=-$ as $t \rightarrow 0$ and both $S_1^+(t)$ and S_2^+ vanish as $(k_B T t)^K$. As a result, $\mathcal{A}(t)$ defined in Eq. (4.44) is dominated by S_1^- in the short time limit and we find

$$|\mathcal{A}(t)| \sim |k_B T t|^{-K} (1 + \dots). \quad (5.3)$$

On the other hand,

$$|\mathcal{B}(t)| = 2|S_2^+(t)| \sim |k_B T t|^K. \quad (5.4)$$

In the long time limit, the numerator of Eq. (4.43) can be approximated for $\zeta=1, 2$ ($S_1^{\tilde{\epsilon}}$ and S_2^+) by

$$\begin{aligned} S_{\zeta}^{\tilde{\epsilon}}(t) &\propto \tilde{\epsilon} e^{-2K\pi|k_B T t|} \int_{R_{\zeta}} d\tilde{t}_1 d\tilde{t}_2 \cos(t - \tilde{t}_1 - \tilde{\epsilon} \tilde{t}_2) \\ &\times C(\tilde{t}_2)^2 \left| \frac{C(\tilde{t}_1)}{C(\tilde{t}_1 - \tilde{t}_2)} \right|^{\tilde{\epsilon}} \end{aligned} \quad (5.5)$$

which vanishes as $e^{-2K\pi|k_B T t|}$ multiplied by an oscillating factor. Also, since the size of the domain R_3 grows with t , S_3^+ and S_3^- become finite and we find

$$\lim_{t \rightarrow \infty} [S_3^+(t) + S_3^-(t)] - 1 = 0. \quad (5.6)$$

Therefore one can expect both $\mathcal{A}(t)$ and $\mathcal{B}(t)$ to vanish exponentially in the long time limit due to thermal fluctuations.

Depending on the relative magnitude of the two energy scales of the problem, namely the Josephson frequency $\omega_0\hbar = e^*V$ and temperature $k_B T$, there may or may not be an intermediate range of times over which both $\mathcal{A}(t)$ and $\mathcal{B}(t)$ show oscillatory behavior. Figure 5 shows the typical time dependence of $\mathcal{A}(\omega_0 t)$ and $\mathcal{B}(\omega_0 t)$ as a function of dimensionless time $\omega_0 t \equiv \tilde{t}$ at high temperatures $\omega_0\hbar \sim k_B T$ and low temperatures $\omega_0\hbar \gg k_B T$.

We can confirm from Fig. 5(a) that when the characteristic time for the exponential decay in the long time limit $(2K\pi k_B T)^{-1}$ [see Eq. (5.5)] is of the same order or less than

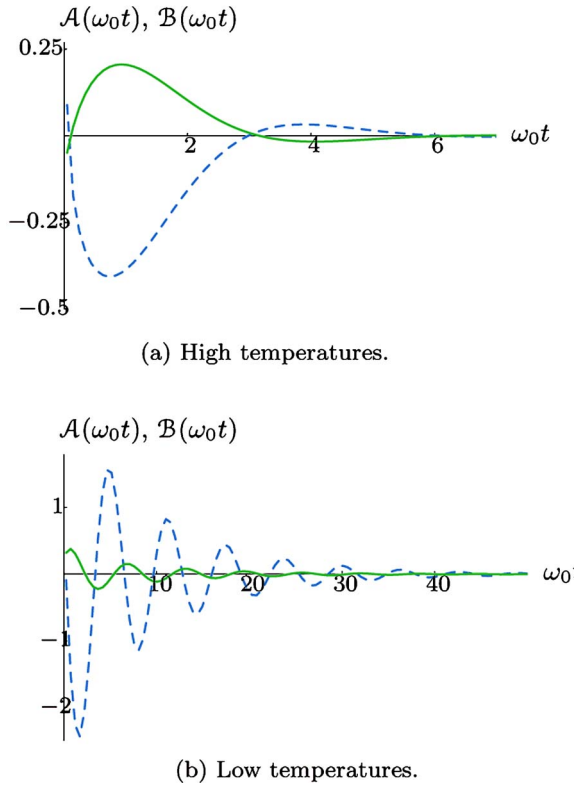


FIG. 5. (Color online) The scaling functions $\mathcal{A}(\omega_0 t)$ (blue dashed line) and $\mathcal{B}(\omega_0 t)$ (green solid line) for $\nu=1/5$ as a function of dimensionless time $\omega_0 t$ at two different temperatures (a) $T/T_0=2$ and (b) $T/T_0=0.25$ where the reference scale is set by the Josephson frequency to be $T_0 \equiv \frac{\omega_0 \hbar}{2\pi k_B}$. $\mathcal{A}(\omega_0 t)$ is dominantly negative at short times due to the divergent contribution coming from counter-current correlations while $\mathcal{B}(\omega_0 t)$ coming only from correlations of currents in the same direction is dominantly positive at short times. $\mathcal{A}(\omega_0 t)$ and $\mathcal{B}(\omega_0 t)$ for other filling factors show similar forms up to an overall scale set by the associated scaling dimension K .

the oscillation period ω_0^{-1} , no oscillations are seen. At the same time, the short time behavior which sets in only for $t \ll (k_B T)^{-1}$ is a less prominent feature of the plot. At moderate time scales, however, $\mathcal{A}(t)$ and $\mathcal{B}(t)$ are of comparable magnitude hence the $\cos \theta$ factor in the “exchange term” of Eq. (4.45) can significantly shift the total noise positively or negatively depending on whether $\theta < \pi/2$ or $\theta > \pi/2$. Hence it is important to understand the intermediate time scale and it can be done so numerically.

For temperatures $T \ll T_0 = \omega_0 \hbar / k_B$, both $\mathcal{A}(t)$ and $\mathcal{B}(t)$ in Fig. 5(b) demonstrate definite oscillatory behavior characterized by the Josephson frequency ω_0 with an exponentially decaying envelope $e^{-K\pi k_B T t}$. Although the magnitude of $\mathcal{B}(t)$ is much smaller than that of $\mathcal{A}(t)$ due to the dominant short-time divergent contributions to $\mathcal{A}(t)$ from S_1^- , one can expect the Fourier spectrum of $\tilde{\mathcal{A}}(\omega)$ and $\tilde{\mathcal{B}}(\omega)$ to show singular behavior in the vicinity of $\omega = \omega_0$. Such features of the Fourier spectrum can be used in experiments to locate the Josephson frequency which is determined by the fractional charge of the FQH QP. In the next section, we discuss the Fourier spectra $\tilde{\mathcal{A}}(\omega)$ and $\tilde{\mathcal{B}}(\omega)$ with a particular interest in

extracting signatures of fractional statistics and fractional charge.

VI. FREQUENCY SPECTRUM $\tilde{S}(\omega)$

As with the time dependent noise, it can be seen from Eq. (4.42) that the frequency spectrum of the normalized noise also gets contributions \tilde{S}_ζ^ϵ from different domains R_ζ as the following:

$$\tilde{S}(\omega) = \int_{-\infty}^{\infty} dt e^{i\omega t} S(t) \equiv \sum_{\zeta=1,3} \sum_{\tilde{\epsilon}=\pm} \tilde{S}_\zeta^\epsilon(\omega) + 2 \cos \theta \tilde{S}_2^+(\omega). \quad (6.1)$$

Noting the fact that the oscillatory time dependence of all $S_\zeta^\epsilon(t)$ comes from the factor $\cos[\omega_0(t-t_1-\tilde{\epsilon}t_2)]$ in Eq. (4.43) ($\tilde{t} \equiv \omega_0 t$), we can use the identity

$$\begin{aligned} \cos[\omega_0(t-t_1-\tilde{\epsilon}t_2)] &= \cos(\omega_0 t) \cos[\omega_0(t_1+\tilde{\epsilon}t_2)] \\ &\quad + \sin(\omega_0 t) \sin[\omega_0(t_1+\tilde{\epsilon}t_2)] \end{aligned} \quad (6.2)$$

to factor out oscillatory factors from each $S_\zeta^\epsilon(t)$ as the following:

$$S_\zeta^\epsilon(t) \propto [\cos(\omega_0 t) \mathcal{F}_\zeta^\epsilon(t) + \sin(\omega_0 t) \mathcal{H}_\zeta^\epsilon(t)], \quad (6.3)$$

where the decaying envelope functions $\mathcal{F}_\zeta^\epsilon(t)$ and $\mathcal{H}_\zeta^\epsilon(t)$ are defined by

$$\begin{aligned} \mathcal{F}_\zeta^\epsilon(t) &\equiv \tilde{\epsilon} \int_{R_\zeta} dt_1 dt_2 \cos[\omega_0(t_1+\tilde{\epsilon}t_2)] \\ &\quad \times [C(\tilde{t}-\tilde{t}_1)C(\tilde{t}_2)]^2 \left[\frac{C(\tilde{t}_1)C(\tilde{t}-\tilde{t}_2)}{C(\tilde{t}_1-t_2)C(\tilde{t})} \right]^\epsilon, \end{aligned} \quad (6.4)$$

$$\begin{aligned} \mathcal{H}_\zeta^\epsilon(t) &\equiv \tilde{\epsilon} \int_{R_\zeta} dt_1 dt_2 \sin[\omega_0(t_1+\tilde{\epsilon}t_2)] \\ &\quad \times [C(\tilde{t}-\tilde{t}_1)C(\tilde{t}_2)]^2 \left[\frac{C(\tilde{t}_1)C(\tilde{t}-\tilde{t}_2)}{C(\tilde{t}_1-t_2)C(\tilde{t})} \right]^\epsilon \end{aligned} \quad (6.5)$$

from Eq. (6.2) and Eq. (4.43).

It is clear from Eq. (6.3) that $\tilde{S}(\omega)_\zeta^\epsilon$ is a convolution of an oscillating part and the envelopes which we may simply compute. Thus we have

$$\begin{aligned} \tilde{S}(\omega)_\zeta^\epsilon &\propto \frac{1}{2} [\tilde{\mathcal{F}}_\zeta^\epsilon(\omega+\omega_0) + \tilde{\mathcal{F}}_\zeta^\epsilon(\omega-\omega_0)] \\ &\quad + \frac{1}{2i} [\tilde{\mathcal{H}}_\zeta^\epsilon(\omega+\omega_0) + \tilde{\mathcal{H}}_\zeta^\epsilon(\omega-\omega_0)], \end{aligned} \quad (6.6)$$

with

$$\tilde{\mathcal{F}}_\zeta^\epsilon(\omega) = \int_{-\infty}^{\infty} dt \tilde{\mathcal{F}}_\zeta^\epsilon(t) e^{i\omega t} = 2 \int_0^{\infty} dt \cos \omega t \tilde{\mathcal{F}}_\zeta^\epsilon(t),$$

$$\tilde{\mathcal{H}}_\zeta^\epsilon(\omega) = \int_{-\infty}^{\infty} dt \tilde{\mathcal{H}}_\zeta^\epsilon(t) e^{i\omega t} = 2i \int_0^{\infty} dt \sin \omega t \tilde{\mathcal{H}}_\zeta^\epsilon(t), \quad (6.7)$$

where we used the fact that $\tilde{\mathcal{F}}_\zeta^\epsilon(t)$ is even in t while $\tilde{\mathcal{H}}_\zeta^\epsilon(t)$ is odd in t . Hence we can understand the frequency spectrum by investigating frequency spectra $\tilde{\mathcal{F}}_\zeta^\epsilon(\omega)$, $\tilde{\mathcal{H}}_\zeta^\epsilon(\omega)$ and superposing them with their centers shifted by $\pm \omega_0$. One important observation to be made in Eq. (6.7) is the fact that $\tilde{\mathcal{F}}_\zeta^\epsilon(\omega)$ is an *even* function of ω while $\tilde{\mathcal{H}}_\zeta^\epsilon(\omega)$ is an *odd* function of ω . As we discussed in the previous section [see Eq. (5.5)], $S_\zeta^\epsilon(t)$ decays exponentially as $e^{-2K\pi k_B T t}$ in the long time limit ($K\pi k_B T t \gg 1$) and hence

$$F_\zeta^\epsilon(t) \sim \mathcal{H}_\zeta^\epsilon(t) \rightarrow e^{-2K\pi k_B T t} \quad (6.8)$$

in the long time limit as well. As a result, the form of $\tilde{\mathcal{F}}_\zeta^\epsilon(\omega)$ is a broadened peak at $\omega=0$ with the width of the peak $2K\pi k_B T$ determined by the temperature and the scaling dimension of FQH QP. Similarly, $\tilde{\mathcal{H}}_\zeta^\epsilon(\omega)$ takes the form of a derivative of a peak with the same width. The characteristic behavior of $\tilde{\mathcal{F}}_\zeta^\epsilon(\omega)$ and $\tilde{\mathcal{H}}_\zeta^\epsilon(\omega)$ is plotted in Fig. 7.

From the definition of the “direct” and “exchange” terms in Eq. (4.44), we can express $\tilde{\mathcal{A}}(\omega)$ and $\tilde{\mathcal{B}}(\omega)$ in terms of $\tilde{\mathcal{F}}_\zeta^\epsilon(\omega)$ and $\tilde{\mathcal{H}}_\zeta^\epsilon(\omega)$ as

$$\begin{aligned} \tilde{\mathcal{A}}(\omega) &= \sum_{\zeta=1,3} \sum_{\tilde{\epsilon}=\pm} \frac{1}{2} [\tilde{\mathcal{F}}_\zeta^\epsilon(\omega_0+\omega;T,K) + \tilde{\mathcal{F}}_\zeta^\epsilon(\omega_0-\omega;T,K)] \\ &\quad + \sum_{\zeta=1,3} \sum_{\tilde{\epsilon}=\pm} \frac{1}{2i} [\tilde{\mathcal{H}}_\zeta^\epsilon(\omega_0+\omega;T,K) - \tilde{\mathcal{H}}_\zeta^\epsilon(\omega_0-\omega;T,K)], \end{aligned} \quad (6.9)$$

$$\begin{aligned} \tilde{\mathcal{B}}(\omega) &= \frac{1}{2} [\tilde{\mathcal{F}}_2^+(\omega_0+\omega;T,K) + \tilde{\mathcal{F}}_2^+(\omega_0-\omega;T,K)] \\ &\quad + \frac{1}{2i} [\tilde{\mathcal{H}}_2^+(\omega_0+\omega;T,K) - \tilde{\mathcal{H}}_2^+(\omega_0-\omega;T,K)]. \end{aligned} \quad (6.10)$$

In the rest of this section, we use the properties of $\tilde{\mathcal{F}}_\zeta^\epsilon(\omega)$ and $\tilde{\mathcal{H}}_\zeta^\epsilon(\omega)$ to understand and discuss $\tilde{\mathcal{A}}(\omega)$ and $\tilde{\mathcal{B}}(\omega)$ in two frequency regimes of interest: low frequency $\omega \ll \omega_0$ and near Josephson frequency $\omega \sim \omega_0$.

For $\omega \ll \omega_0$, both $\tilde{\mathcal{A}}(\omega)$ and $\tilde{\mathcal{B}}(\omega)$ collect tail ends of shifted $\tilde{\mathcal{F}}_\zeta^\epsilon(\omega)$ and $\tilde{\mathcal{H}}_\zeta^\epsilon(\omega)$. Naturally, they show white noise behavior and hence we focus on zero frequency values $\tilde{\mathcal{A}}(\omega=0) \equiv \tilde{\mathcal{A}}_0$ and $\tilde{\mathcal{B}}(\omega=0) \equiv \tilde{\mathcal{B}}_0$ which depend only on the temperature (see Fig. 6). The direct term $\tilde{\mathcal{A}}_0$ is negative due to its dominant contributions coming from $\tilde{\epsilon}=-$ processes in domain R_1 with the opposite orientation of the currents as illustrated in case O of Fig. 3. On the other hand, $\tilde{\mathcal{B}}_0$ is positive as it only involves case S($\tilde{\epsilon}=+$) from domain R_2 . As a result, Eq. (4.45) translates to

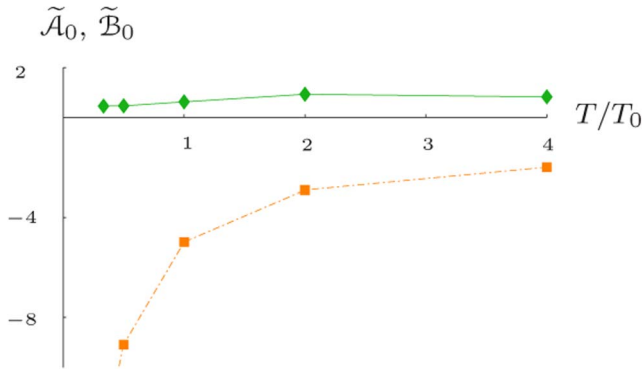


FIG. 6. (Color online) A typical temperature dependence of zero frequency values of the direct term $\tilde{A}(\omega=0)$ (orange dashed line) and the exchange term $\tilde{B}(\omega=0)$ (green solid line) taken from $\nu=2/5$ case. The exchange contribution $\tilde{B}(\omega=0)$ is comparable to the direct term in the temperature range $2 \leq T/T_0 \leq 4$ and hence the fractional statistics has a marked effect on the total noise at small frequencies in the same temperature range. The qualitative behavior is universal to all fractions.

$$\tilde{S}(\omega=0) = -|\tilde{A}_0| + \cos \theta |\tilde{B}_0| \quad (6.11)$$

for the frequency spectrum of the noise at zero frequency. At low temperatures ($T \ll T_0$, $T_0 \equiv \hbar\omega_0/k_B \sim 80$ mK for $V=40$ μ V), $|\tilde{A}_0|$ dominates the spectrum since contributions from $\tilde{\mathcal{H}}_1^-(\omega_0)$ and $\tilde{\mathcal{F}}_1^-(\omega_0)$ both diverges in the $T \rightarrow 0$ limit displaying T^{-K} power law divergence. However at higher temperatures, both $\tilde{\mathcal{F}}_\zeta^-(\omega)$ and $\tilde{\mathcal{H}}_\zeta^-(\omega)$ are more similar to a Lorenzian for all ζ and ϵ . Hence for temperatures of order T_0 , \tilde{B}_0 is comparable to \tilde{A}_0 as we display in Fig. 6. (At even higher temperatures, both correlations are washed out by thermal fluctuations.) Consequently the statistics dependent exchange contribution $\cos \theta |\tilde{B}_0|$ will noticeably affect the experimental measurement of the total noise at small frequencies at such temperatures. It is rather astonishing that the statistical angle θ , which was originally quantum mechanically defined in a highly theoretical basis, can be measured in this reasonably accessible frequency range at finite temperature.

Near the Josephson frequency, \tilde{A} and \tilde{B} develop qualitatively different sharp features at temperatures $T \ll T_0/K$: $\tilde{A}(\omega)$ nearly crosses ω axis steeply while $\tilde{B}(\omega)$ develops a peak of width $2Kk_B T/\hbar$. This can be understood by analyzing which terms among $\tilde{\mathcal{F}}_\zeta^-(\omega)$ and $\tilde{\mathcal{H}}_\zeta^-(\omega)$ dominate each of $\tilde{A}(\omega)$ and $\tilde{B}(\omega)$. As for \tilde{A} , its dominant contribution is from domain R_1 with $\zeta=-$. Further, $i\tilde{\mathcal{H}}_1^-(\omega)$ is strongly dominant over $\tilde{\mathcal{F}}_1^-(\omega)$ in magnitude as can be reasoned as below.

Recalling from Eq. (6.5) that $\tilde{\mathcal{F}}_1^-(\omega)$ and $i\tilde{\mathcal{H}}_1^-(\omega)$ have $\cos[\omega_0(t_1-t_2)]|\sinh[\pi k_B T(t_1-t_2)]|^{-K}$ and $\sin[\omega_0(t_1-t_2)]|\sinh[\pi k_B T(t_1-t_2)]|^{-K}$ factors in their integrands respectively, each of their characteristic behaviors can be captured by $\int_0^\infty dt' \cos t' |\sinh(\pi k_B T t')|^{-K}$ and

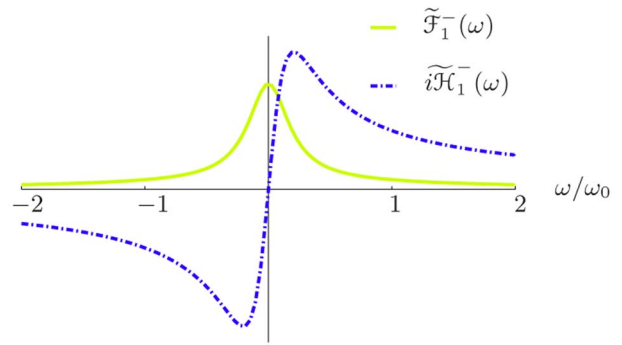


FIG. 7. (Color online) Two dominant contributions to \tilde{A} as a function of ω/ω_0 at temperature $T=0.5T_0$: $\tilde{\mathcal{F}}_1^-(\omega)$ in (green) solid line and $i\tilde{\mathcal{H}}_1^-(\omega)$ in (blue) dotted line. The width of the peaks is $2Kk_B T$. $i\tilde{\mathcal{H}}_1^-(\omega)$ is already dominant with a stronger contribution at the tail, even at this temperature. As the temperature is further decreased, the dominance of $i\tilde{\mathcal{H}}_1^-(\omega)$ over $\tilde{\mathcal{F}}_1^-(\omega)$ becomes even more prominent.

$\int_0^\infty dt' \sin t' |\sinh(\pi k_B T t')|^{-K}$ with the latter dominating over the former for $(K\pi k_B T) \ll 1$.

Comparison between $\tilde{\mathcal{F}}_1^-(\omega)$ and $i\tilde{\mathcal{H}}_1^-(\omega)$ plotted in Fig. 7, this observation and hence $\tilde{A}(\omega)$ in the vicinity of $\omega=\omega_0$ can be approximated as

$$\tilde{A}(\omega) \approx \frac{i}{2} \tilde{\mathcal{H}}_1^-(\omega_0 - \omega) \quad (6.12)$$

plus small corrections from other contributions including the tail of the same function centered around $\omega=-\omega_0$: $\tilde{\mathcal{H}}_1^-(\omega_0 + \omega)$. Since $\tilde{\mathcal{H}}_\zeta^-(\omega)$ is an odd function of ω as we mentioned earlier, the dominant contribution from $\tilde{\mathcal{H}}_1^-(\omega_0 - \omega)$ to $\tilde{A}(\omega)$ makes it nearly cross the ω axis in the vicinity of the Josephson frequency; thus suppressing the contribution of $\tilde{A}(\omega_0)$ to the total noise.

We now turn to \tilde{B} which determines the magnitude of the “exchange” term that bears the statistical angle dependence. Given that only domain R_2 , $\zeta=+$ contributes to \tilde{B} , the parts of the integrands that strictly depend only on t_1 and t_2 now become $\cos[\omega_0(t_1+t_2)]|\sinh[\pi k_B T(t_1-t_2)]|^K$ and $\sin[\omega_0(t_1+t_2)]|\sinh[\pi k_B T(t_1-t_2)]|^K$, respectively for $\tilde{\mathcal{F}}_2^+(\omega)$ and $\tilde{\mathcal{H}}_2^+(\omega)$. Since the argument of the trigonometric function is the sum (t_1+t_2) , while the difference (t_1-t_2) enters the sinh function in a nonsingular fashion, both $\tilde{\mathcal{F}}_2^+(\omega)$ and $\tilde{\mathcal{H}}_2^+(\omega)$ are of comparable magnitude away from their centers $\omega=0$ [where $\tilde{\mathcal{F}}_2^+(\omega=0) \neq 0$ (even function), while $\tilde{\mathcal{H}}_2^+(\omega=0)=0$ (odd function)]. Thus, $\tilde{B}(\omega \sim \omega_0)$ can be appropriately approximated as

$$\tilde{B}(\omega) \approx \tilde{\mathcal{F}}_2^+(\omega_0 - \omega), \quad (6.13)$$

which has a peak centered at $\omega=\omega_0$.

From the preceding analysis, we can conclude that the exchange term plays a significant role in the measured net correlation $\tilde{S}(\omega/\omega_0=1)$ by shifting it to a positive (negative)

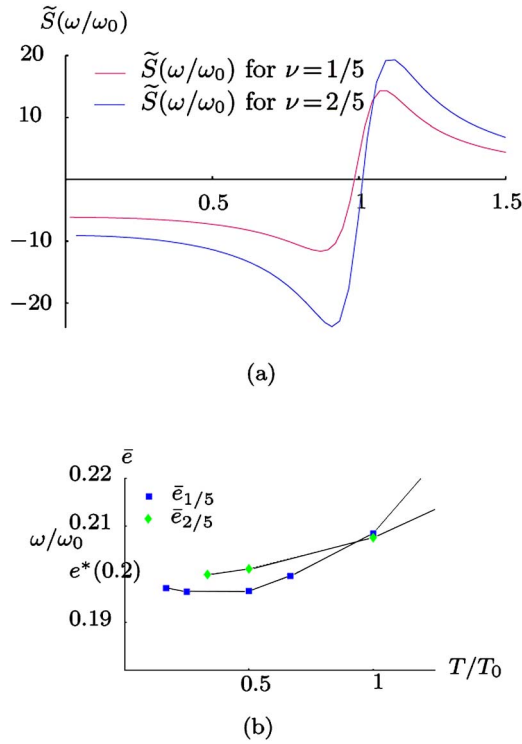


FIG. 8. (Color online) (a) $\tilde{S}(\omega/\omega_0)$ for $\nu=1/5$ and $2/5$ for $T=20, 40$ mK, respectively, with $V \sim 40$ μ V. $\tilde{S}(\omega/\omega_0)$ shows a peak in the vicinity of the Josephson frequency ω_0 . At ω_0 , $\tilde{S}(\omega/\omega_0=1)$ is positive for the Laughlin state $\nu=1/5$ and negative for the Jain state $\nu=2/5$. (b) The effective charge $\bar{e}(T)$ in units of e is determined by the crossing points of (a) for $\nu=1/5$ and $2/5$.

value for Laughlin (non-Laughlin) states since the exchange term has $\cos \theta > 0$ ($\cos \theta < 0$), and the direct term $\tilde{\mathcal{A}}(\omega)$ is strongly suppressed near the Josephson frequency. These sharp features not only provide a direct measurement of the fractional charge associated with the Josephson frequency, but also allow a natural contrast between two filling factors with the same charge but different statistics, e.g., $\nu=1/5$ and $\nu=2/5$, as we show in Fig. 8(a). The information on statistics and charge contained in the noise near the Josephson frequency is recapitulated in Fig. 8(b) by introducing an effective charge $\bar{e} = \hbar \bar{\omega} / V$ from the crossing point of \tilde{S} , i.e., $\tilde{S}(\bar{\omega}/\omega_0)=0$. The deviation between \bar{e} for $\nu=1/5$ and $\nu=2/5$ —satisfying $\bar{e}_{1/5} < e^* < \bar{e}_{2/5}$ over a broad temperature range despite their common fractional charge $e^* = e/5$ —is a consequence of different statistical angles $\theta = \pi/5$ (bunching) for $\nu=1/5$ and $\theta = 3\pi/5$ (antibunching) for $\nu=2/5$. Observation of such deviation will be a definite signature for the existence of anyons.

We conclude this section by summing up the two main results which show ways to extract the effect of fractional statistics $\tilde{S}(\omega=0) = -|\tilde{\mathcal{A}}_0| + \cos \theta |\tilde{\mathcal{B}}_0|$ for the zero frequency Fourier spectrum plotted in Fig. 6; e^* defined from $\tilde{S}(\omega)$ for ω near Josephson frequency. The first result can be used to measure the statistical angle in a quantitative manner while the second result can be used to determine the $\text{sgn}(\cos \theta)$ and hence detect bunching versus antibunching behavior.

VII. CONCLUDING REMARKS AND MULTI-TERMINAL NOISE EXPERIMENTS

In summary, we have shown that the cross-current noise in a T junction can be used to directly measure the statistical angle θ independently from the fractional charge, and conceptually, from the filling factor ν . The normalized cross-current noise as a function of frequency ω assumes the form of a scaling function that depends on the quantities ω/ω_0 and $\hbar\omega_0/kT$, where ω_0 is the Josephson frequency, and all the statistical dependence is contained in a simple $\cos \theta$ factor. The low frequency results show that there is a quantitatively significant statistics dependence of this noise. We have also shown how to measure both fractional charge and statistics near the Josephson frequency. Specifically, since the Josephson frequency explicitly depends on the fractional charge, identifying its approximate value based on where the finite frequency cross-current noise drops to zero would provide a means of measuring fractional charge. It must be noted that the fractional charge, being a single-particle property, can be detected through autocurrent correlations, i.e., shot noise measurements. The zero frequency shot noise is proportional to the fractional charge in the weak tunneling limit^{12–14,31} while the finite frequency shot noise shows a peak at the Josephson frequency.²⁵

Plotting the actual frequency at which the cross-current noise drops to zero as a function of temperature and comparing this value to the expected Josephson frequency would give a measure of the bunching versus antibunching behavior of the QP's arising from statistics. A definitive means of measuring such statistical behavior would be by comparing the cross-current noise of two FQH states with the same fractional charge but different fractional statistics, thus pinpointing the effect of topological order. We remark that our results are independent of nonuniversal short time physics.

In this paper, we have considered a setup, the T junction, consisting of quantum Hall bar with three terminals. In this setup, two quasiparticles (or a quasiparticle-quasi-hole pair) are created (or destroyed) at nearby places of one terminal (terminal 0 in Fig. 2). In the final state the two other terminals (1 and 2 in Fig. 2), which are widely separated, each detects just one quasiparticle. We have assumed throughout that the two quasiparticles are created at nearby points in terminal 0 separated by a distance a small compared with the magnetic length. Our calculation can be straightforwardly generalized for the situation in which a is somewhat greater than the magnetic length. However, as a increases, various decoherence effects will hinder the detection of the statistical phase. In particular, when $a \gtrsim v\hbar/k_B T$, where v is the speed of the propagating charge mode, thermal fluctuation will overwhelm the coherent propagation of edge state between two points, and the interference effects associated with fractional statistics will become rapidly unobservable.

Safi *et al.*²² have recently considered the identical setup for Laughlin states at $T=0$ and obtained a series expression for $\tilde{S}(\omega=0)$ for the case O alone as a function of ν (note that for Laughlin states one cannot distinguish ν from K or e^*/e or θ/π). Indeed, our finite temperature calculation shows that the total cross current noise will be completely domi-

nated by case O as $T \rightarrow 0$ which was the case of interest in Ref. 22. However, our study also shows that, at finite temperatures, case S brings in an explicit statistics dependence in the form of $\cos \theta$ which can be distinguished from the effect of the fractional charge and the scaling dimension for non-Laughlin states. Furthermore, even at relatively low temperature at which most noise experiments involving QH systems take place (see below), this statistics dependent contribution was found to be of comparable magnitude as the statistics independent contribution. It is rather encouraging to find that a purely quantum mechanical property such as statistics can in principle be observed in our setup at nonzero temperatures. In fact it is precisely the finite temperature that assists processes that are sensitive to statistics. A closely related setup is the four terminal case studied (only for Laughlin states at $T=0$) by Vishveshwara in Ref. 29, where the cross current noise at equal times $t=0$ was calculated for the contribution that involves all four terminals. We should note, however, that even in this case, an actual measurement of the cross-correlation will have contributions from correlation between three of the four terminals which is precisely $S(t)$ we have calculated here. A number of interesting interferometers have been proposed to detect fractional statistics,^{32–35} none of which has yet been realized experimentally, except possibly for the recent experiments of Refs. 36–38. Theoretical schemes to measure non-Abelian statistics have also been proposed.^{39,40}

Here we have presented the calculation using the edge state theory constructed by Lopez and Fradkin for Jain states.¹⁷ However, as long as one can limit oneself to a single propagating mode by either choosing the most relevant mode of hierarchical picture (see below) or by using Lopez-Fradkin picture which only has one propagating mode by design, the theory presented here is applicable and could indeed be used to compare predictions from different descriptions.

For the T -junction setup studied here, the hierarchical picture would imply multiple propagating edge modes for non-Laughlin states. In Ref. 10, Wen derived the effective theory for edge states of hierarchical FQH states following Haldane's hierarchical construction.⁴¹ According to the hierarchical theory, the $\nu=2/5$ FQH state is generated by the condensation of quasiparticles on top of the $\nu=1/3$ FQH state. Thus the $2/5$ state contains two components of incompressible fluids. If we consider a special edge potential such that the FQH state consists of two droplets, then in this picture, one is the electron condensate with a filling fraction $\nu_1=1/3$ and radius r_1 , and the other is the quasiparticle condensate (on top of the $1/3$ state) with a filling fraction $\nu_2=1/15$ (note $1/3+1/15=2/5$) and radius $r_2 < r_1$. Recently, one of us used this picture⁴² to account for the superperiod Aharonov-Bohm oscillations observed in recent experiments,^{36–38} where the smooth edge potential could indeed have created two droplet situation. On the other hand, if the edge is sharply defined so that there can be direct tunneling between descendant states ($2/5$ state, for example), it is reasonable to consider the tunneling current being dominantly carried by the mode which has the smallest scaling dimension (that is “most” relevant in the renormalization group sense). In Wen's theory, although the primary edge QP

mode carries $e^*=1/5$, $\theta/\pi=K=3/5$, it is actually the QP mode with $e^*=\theta/\pi=K=2/5$ that is most relevant,¹⁰ which is quite different from the $e^*=1/5$, $\theta/\pi=3/5$, $K=1/10$ for the charge mode in Lopez-Fradkin picture. In fact, given that our calculation is applicable to alternate pictures which come with different predictions, an experiment such as the one proposed here, where the charge and statistics of Jain state quasiparticles can separately be identified, becomes all the more immediate.

Turning to experiments, some recent measurements in a quantum interferometer geometry were interpreted to imply fractional statistics. An effective charge extracted in recent shot noise experiments⁴³ was somewhat larger than the minimum quasiparticle charge, suggesting bunching behavior. Observation of Aharonov-Bohm oscillations with a superperiod in an antidot^{36–38} have also been ascribed to statistical effects. However, the noise measurements we propose here will allow for a direct and independent way of measuring both fractional statistics and charge separately. Low frequency prediction have the advantage of yielding quantitatively significant statistics dependence of the noise. Near the Josephson frequency, our prediction has the strength of probing both charge and statistics simultaneously. The geometry proposed and the required experimental conditions are all very much within current capabilities. The T -junction setup is reminiscent of the multilead geometry employed in effective charge measurement, though, the issue of whether or not the fabricated T junction would form a single point contact would be relevant. Typical parameters used in noise experiments^{14,43} are bias voltages of $10\text{--}150\text{ }\mu\text{V}$ (corresponding to a Josephson frequency $\omega_0 \sim 1\text{ GHz}$), and temperatures of $10\text{--}100\text{ mK}$. These parameters access the ratios of T/T_0 shown here, making our proposal plausible. The parameter regime in which the perturbative results for cross-current correlations are valid depends on the interedge tunneling amplitude and consequently on fabrication. The condition (on applied voltage and temperature) for remaining in this regime is that the ratio between tunneling current and maximum edge state current ne^2V/h be small, i.e., of order 0.1.

A definitive measurement of anyonic statistics, such as the one proposed here, would be one of the first instances of experimentally establishing the existence of topological order.^{10,19} Employing topological order has recently emerged as a possible route to decoherence free quantum computing.⁴⁴ Clear signatures of fractional statistics would mark the very first steps towards bringing some of these fascinating ideas to life.

ACKNOWLEDGMENTS

This work was supported in part by the National Science Foundation through Grant Nos. DMR 04-42537 (E.K., M.L., E.F.), DOE-MRL DEFG02-91-ER45439 (S.V.), by the Research Board of the University of Illinois (E.F., M.L.), and by a Stanford Institute for Theoretical Physics (E.K.). We thank F.D.M. Haldane for illuminating discussions regarding exclusion statistics in the setup of this paper and C. Chamon for many helpful comments (particularly on Klein factors).

We also thank M. Heiblum and C. Marcus for discussions on noise experiments. We thank E. Ardonne for many helpful discussions.

APPENDIX A: CHIRAL AND NONCHIRAL BOSON COMMUTATION RELATIONS AND CORRELATION FUNCTIONS

In this appendix we quantize the chiral boson theory and calculate its correlation function. We also extend this calculation to the case of a neutral topological field that is non-propagating.

The Lagrangian density for a left/right moving free massless chiral boson field $\phi_{\pm}(x \pm vt)$ propagating with speed v is

$$\mathcal{L}_{\pm} = \frac{g}{4\pi} \partial_x \phi_{\pm} (\pm \partial_t \phi_{\pm} - v \partial_x \phi_{\pm}) \quad (\text{A1})$$

with the corresponding action $S_0 = \int d^2r \mathcal{L}$, where $\vec{r} = (x, t)$ and g is a positive real parameter. Notice that the Lagrangian is invariant under an arbitrary overall shift of the field ϕ_{\pm} , i.e.,

$$\mathcal{L}_{\pm}[\phi_{\pm}(\vec{r})] = \mathcal{L}_{\pm}[\phi_{\pm}(\vec{r}) + \alpha] \quad (\text{A2})$$

with an arbitrary constant α . Hence \mathcal{L}_{\pm} is independent of the zero mode of ϕ_{\pm} .

Correct quantization of these chiral bosons can be achieved by the following equal time commutation relations

$$\left[\phi_{\pm}(x, t), \pm \frac{g}{4\pi} \partial'_x \phi_{\pm}(x', t) \right] = \frac{1}{2} i \delta(x - x'), \quad (\text{A3})$$

where the factor of $\frac{1}{2}$ comes from the fact that ϕ_{\pm} are non-local fields with respect to the nonchiral boson $\phi \equiv \phi_{+} + \phi_{-}$ occupying only half the phase space of ϕ . The nonchiral boson ϕ is a true local field and it can be quantized in the usual way. We will find below that Eq. (A3) is indeed the correct commutation relations consistent with the commutation relations of nonchiral boson. To find the nonchiral boson Lagrangian using a path integral, we need another (dual) nonchiral bosonic field θ to change the basis from ϕ_{-} and ϕ_{+} to ϕ and θ . Hence we define

$$\theta \equiv \phi_{-} - \phi_{+} \quad (\text{A4})$$

and write ϕ_{\pm} in terms of ϕ and θ as the following:

$$\phi_{+} = \frac{1}{2}(\phi - \theta), \quad \phi_{-} = \frac{1}{2}(\phi + \theta). \quad (\text{A5})$$

Then the total Lagrangian for two fields can be written in terms of ϕ and θ as

$$\mathcal{L}_{+} + \mathcal{L}_{-} = -\frac{g}{8\pi} [\partial_x \phi \partial_t \theta + \partial_x \theta \partial_t \phi + v(\partial_x \phi)^2 + v(\partial_x \theta)^2] \quad (\text{A6})$$

and the path integral for two chiral fields can be written as a path integral for two nonchiral fields to give

$$\begin{aligned} Z &= \int \mathcal{D}\phi_{-} \int \mathcal{D}\phi_{+} e^{i \int d^2r [\mathcal{L}_{+}[\phi_{\pm}] + a\phi_{\pm}]} \\ &= \int \mathcal{D}\phi \int \mathcal{D}\theta e^{-i(g/8\pi) \int d^2r [v(\partial_x \theta)^2 + 2\partial_t \phi \partial_x \theta + v(\partial_x \phi)^2]}. \end{aligned} \quad (\text{A7})$$

Now we can integrate θ out from the above equation

$$Z = \int \mathcal{D}\phi e^{i \int d^2r (g/8\pi) [1/v(\partial_t \phi)^2 - v(\partial_x \phi)^2]} \quad (\text{A8})$$

to obtain the Lagrangian for the nonchiral field ϕ

$$\mathcal{L}[\phi] = \frac{g}{8\pi} \left[\frac{1}{v} (\partial_t \phi)^2 - v(\partial_x \phi)^2 \right]. \quad (\text{A9})$$

We can find the canonical conjugate of ϕ , Π_{ϕ} in the usual way to be

$$\Pi_{\phi} = \frac{\delta \mathcal{L}}{\delta \partial_t \phi} = \frac{1}{v} \frac{g}{4\pi} \partial_t \phi \quad (\text{A10})$$

with the equal time commutation relation

$$[\phi(x), \Pi_{\phi}(x')] = i \delta(x - x'). \quad (\text{A11})$$

However, since $\phi = \phi_{-}(x - vt) + \phi_{+}(x + vt)$

$$\partial_t \phi = \partial_t(\phi_{-} + \phi_{+}) = -v \partial_x(\phi_{-} + \phi_{+}) = -v \partial_x \theta \quad (\text{A12})$$

which means $\partial_x \theta$ is proportional to the canonical conjugate Π_{ϕ} :

$$\Pi_{\phi} = -\frac{g}{4\pi} \partial_x \theta \quad (\text{A13})$$

and hence Eq. (A11) can be rewritten as

$$[\phi(x), \partial_x \theta(x')] = -i \frac{4\pi}{g} \delta(x - x'). \quad (\text{A14})$$

From Eqs. (A5) and (A14) one can check that Eq. (A3) indeed is the correct way of quantizing the chiral modes.

Now integrating both sides of Eq. (A3) with respect to $x' - x$ and noting that $\partial_{x'}[\phi_{\pm}(x), \phi_{\pm}(x')] = [\phi_{\pm}(x), \partial_{x'} \phi_{\pm}(x')] - [\partial_{x'} \phi_{\pm}(x), \phi_{\pm}(x')]$, one finds the following equal time commutation relations for left/right moving bosons ϕ_{\pm}

$$[\phi_{+}(x), \phi_{+}(x')] = -i \frac{\pi}{g} \text{sgn}(x - x'),$$

$$[\phi_{-}(x), \phi_{-}(x')] = i \frac{\pi}{g} \text{sgn}(x - x'). \quad (\text{A15})$$

To calculate the chiral boson propagator, we first define a generating functional

$$\begin{aligned} Z[a] &= \int \mathcal{D}\phi_{\pm} e^{i \int d^2r [\mathcal{L}_{\pm}[\phi_{\pm}] + a\phi_{\pm}]} \\ &= Z[0] e^{-(1/2) \int d^2r \int d^2r' a(r) M_{\pm}^{-1}(r - r') a(r')}, \end{aligned} \quad (\text{A16})$$

where we defined the differential operator associated with the Lagrangian \mathcal{L}_{\pm}

$$M_{\pm} \equiv i \frac{g}{2\pi} \partial_x (\pm \partial_t - v \partial_x). \quad (\text{A17})$$

Now the propagator is nothing but the inverse of M since

$$\begin{aligned} G_{\pm}(\vec{r} - \vec{r}') &= \langle \phi_{\pm}(\vec{r}) \phi_{\pm}(\vec{r}') \rangle = - \left. \frac{\delta \ln Z[a]}{\delta a(\vec{r}) \delta a(\vec{r}')} \right|_{a=0} \\ &= M_{\pm}^{-1}(\vec{r} - \vec{r}'), \end{aligned} \quad (\text{A18})$$

and can be calculated using a Fourier transformation with the proper epsilon prescription for a time ordered propagator [substituting ω with $\omega + i\epsilon \operatorname{sgn}(\omega)$ in the limit $\epsilon \rightarrow 0^+$]:

$$\begin{aligned} G_{\pm}(\vec{r}) &= \int \frac{dk d\omega}{(2\pi)^2} \frac{e^{i(kx-\omega t)}}{ig ik \{ \mp i[\omega + i\epsilon \operatorname{sgn}(\omega)] - ivk \}} \\ &= i \int \frac{dk d\omega}{2\pi} \frac{1}{g k [\omega + i\epsilon \operatorname{sgn}(\omega) - vk]} e^{-i(\omega t \pm x)} \\ &= \frac{1}{g} \int \frac{dk}{k} [e^{-ik(vt \pm x) - k\tau_0} \Theta(k) \Theta(t) \\ &\quad - e^{ik(vt \pm x) + k\tau_0} \Theta(-k) \Theta(-t)]. \end{aligned} \quad (\text{A19})$$

Here we introduced a UV (short distance) cutoff τ_0 and used the fact that the ω contour integral has to be closed in the lower (upper) half plane for $t > 0$ ($t < 0$) and $\operatorname{sgn}(\omega) = \operatorname{sgn}(k)$ near the pole at $\omega = vk$. Notice that the left (right) moving propagator G_+ (G_-) indeed depends only on $vt+x$ ($vt-x$), i.e., $\phi_{\pm}(x, t) = \phi_{\pm}(vt \pm x)$. It is clear from Eq. (A19) that $G(r)$ has a logarithmic divergence in the small k (IR) limit. However, one can define a finite quantity by subtracting the equal position propagator $G(0)$, which also has a logarithmic divergence, and obtain the following:

$$\begin{aligned} \tilde{G}_{\pm}(\vec{r}) &\equiv G_{\pm}(\vec{r}) - G_{\pm}(0) \\ &= \frac{1}{g} \int \frac{dk}{k} [\{e^{-ik(vt \pm x) - k\tau_0} - 1\} \Theta(k) \Theta(t) \\ &\quad - \{e^{ik(vt \pm x) + k\tau_0} - 1\} \Theta(-k) \Theta(-t)] \\ &= -\frac{1}{g} \ln \left[\frac{\tau_0 + i \operatorname{sgn}(t)(vt \pm x)}{\tau_0} \right]. \end{aligned} \quad (\text{A20})$$

At finite temperatures T , the regulated and time ordered propagator can be calculated from Eq. (A20) via conformal mapping to take the following form:

$$\tilde{G}_{\pm}(x', t) = -\frac{1}{g} \ln \left[\frac{\frac{\pi}{\beta} \tau_0}{\sin \left[\frac{\pi \tau_0}{\beta} + i \operatorname{sgn}(t) \frac{\pi}{\beta} (vt \pm x) \right]} \right], \quad (\text{A21})$$

where $\beta = 1/(k_B T)$ is the inverse temperature with k_B being the Boltzmann constant.

In the nonpropagating limit of $v_N \rightarrow 0^+$, Eq. (A1) becomes the Lagrangian for a topological field^{17,45} as the following:

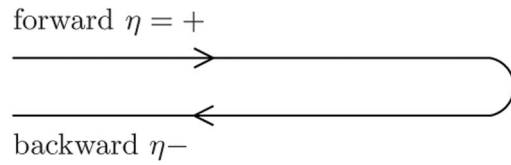


FIG. 9. The Keldysh contour from $t = -\infty$ to $t = \infty$ along the forward branch ($\eta = +$), and back to $t = -\infty$ along the backward branch ($\eta = -$).

$$\mathcal{L}_N = \frac{g_N}{4\pi} \partial_x \phi_N \partial_t \phi_N, \quad (\text{A22})$$

where g_N can be either positive or negative real number. \mathcal{L}_N is still invariant under an arbitrary overall shift of the topological field ϕ_N and the propagator for the topological field can be calculated in the similar way as for the chiral field:

$$\begin{aligned} \langle T \phi_N(\vec{r}) \phi_N(0) \rangle &= -\frac{i}{g_N} \int \frac{dk d\omega}{2\pi} \frac{e^{i(kx-\omega t)}}{k\omega} \\ &= -\frac{i}{g_N} \frac{1}{2\pi} [-i\pi \Theta(t) + i\pi \Theta(-t)] \\ &\quad \times [i\pi \Theta(x) - i\pi \Theta(-x)] \\ &= -\frac{i}{g_N} \frac{\pi}{2} \operatorname{sgn}(t) \operatorname{sgn}(x) \\ &= \lim_{v_N \rightarrow 0^+} \frac{i}{g_N} \frac{\pi}{2} \operatorname{sgn}(t) \operatorname{sgn}(v_N t + x), \end{aligned} \quad (\text{A23})$$

where the limit should be taken at the end of any calculation that uses $\langle \phi_N(\vec{r}) \phi_N(0) \rangle$.

APPENDIX B: CONTOUR ORDERED (KELDYSH) PROPAGATORS FOR CHIRAL BOSONS

Here we derive the contour ordered Green functions for chiral bosons described by the Lagrangian (A1) and topological modes described by Eq. (A22). Time ordered propagator can be thought of as a sum of two terms depending on the sign of $(t-t')$:

$$\begin{aligned} \langle T \phi(x, t) \phi(x', t') \rangle &= \Theta(t-t') \langle \hat{\phi}(x, t) \hat{\phi}(x', t') \rangle \\ &\quad + \Theta(t'-t) \langle \hat{\phi}(x', t') \hat{\phi}(x, t) \rangle. \end{aligned} \quad (\text{B1})$$

In the same way, a contour ordered propagator is determined by the order in which different times appear on the contour sketched in Fig. 9

$$\begin{aligned} G_{\eta, \eta'}(x - x', t - t') &= \langle T_K \phi(x, t^\eta) \phi(x', t'^{\eta'}) \rangle \\ &\equiv \begin{cases} \langle \phi(x, t^\eta) \phi(x', t'^{\eta'}) \rangle & \text{for } t^\eta >_K t'^{\eta'}, \\ \langle \phi(x', t'^{\eta'}) \phi(x, t^\eta) \rangle & \text{for } t'^{\eta'} >_K t^\eta, \end{cases} \end{aligned} \quad (\text{B2})$$

where we used the expression $t >_K t'$ to denote t appearing later than t' in the contour. Clearly when both times occur in

the forward branch ($\eta=\eta'=+$), contour ordering is the same as time ordering and when both times occur in the backward branch ($\eta=\eta'=-$), contour ordering is the same as antitime ordering. On the other hand, when t is on the backward branch while t' is on the forward branch ($\eta=-$, $\eta'=+$), obviously t is occurring later in the contour and the exact opposite is the case for $\eta=+$, $\eta'=-$. Comparing the time ordered propagator (A20) with Eq. (B1) and setting $v=1$

$$\langle \hat{\phi}_{\pm}(x,t) \hat{\phi}_{\pm}(0,0) \rangle = -\frac{1}{g} \ln \left[\frac{\tau_0 + i(t \pm x)}{\tau_0} \right] \quad (\text{B3})$$

and combining this with the above observation, we arrive at the following contour ordered propagators for the right moving chiral boson ϕ_- :

$$G_{-+}(x,t) = \langle \phi_-(x,t) \phi_-(0,0) \rangle = \frac{1}{g} \ln \left[\frac{\tau_0 + i(t-x)}{\tau_0} \right],$$

$$G_{+-}(x,t) = \langle \phi_-(0,0) \phi_-(x,t) \rangle = \frac{1}{g} \ln \left[\frac{\tau_0 - i(t-x)}{\tau_0} \right],$$

$$G_{++}(x,t) = \langle T\phi_-(x,t) \phi_-(0,0) \rangle = \frac{1}{g} \ln \left[\frac{\tau_0 + i \operatorname{sgn}(t-0)(t-x)}{\tau_0} \right],$$

$$G_{--}(x,t) = \langle T\phi_-(0,0) \phi_-(x,t) \rangle = \frac{1}{g} \ln \left[\frac{\tau_0 - i \operatorname{sgn}(t)(t-x)}{\tau_0} \right], \quad (\text{B4})$$

which can be written in the following compact form:

$$G_{\eta,\eta'}(x,t) = -\frac{1}{g} \ln \left[\frac{\tau_0 + i \chi_{\eta,\eta'}(t)(t-x)}{\tau_0} \right], \quad (\text{B5})$$

where we introduced

$$\chi_{\eta,\eta'}(t) \equiv \frac{\eta + \eta'}{2} \operatorname{sgn}(t) - \frac{\eta - \eta'}{2}. \quad (\text{B6})$$

Going through the similar analysis for the neutral mode we derive the following contour ordered propagator

$$G_{\eta,\eta'}^N(x,t) = \lim_{v_N \rightarrow 0} -i \frac{\pi}{2} \chi_{\eta,\eta'}(t) \operatorname{sgn}(v_N t - x). \quad (\text{B7})$$

Notice that both $G_{-+}(x,0) - G_{+-}(x,0)$ and $G_{-+}^N(x,0) - G_{+-}^N(x,0)$ properly yield appropriate commutation relations for ϕ_- and ϕ_N as one would expect. At finite temperatures, Eq. (B5) becomes

$$G_{\eta,\eta'}(x,t) = -\frac{1}{g} \ln \left[\frac{\sin \left(\frac{\pi \tau_0}{\beta} + i \chi_{\eta,\eta'}(t) \frac{\pi}{\beta} (t-x) \right)}{\frac{\pi \tau_0}{\beta}} \right]. \quad (\text{B8})$$

However, since the neutral mode is a nonpropagating mode its propagator is independent of the temperature.

Finally, in the limit of $x \rightarrow 0^-$ and $\tau \rightarrow 0$, Eqs. (B8) and (B7) becomes

$$\begin{aligned} G_{\eta,\eta'}(0^-,t) &= -\frac{1}{g} \ln \left| \frac{\sinh \frac{\pi t}{\beta}}{\frac{\pi \tau_0}{\beta}} \right| - i \frac{1}{g} \frac{\pi}{2} \chi_{\eta,\eta'}(t) \operatorname{sgn}(t), \\ G_{\eta,\eta'}^N(0^-,t) &= \lim_{v_N \rightarrow 0^+} \left[-i \frac{1}{g} \frac{\pi}{2} \chi_{\eta,\eta'}(t) \operatorname{sgn}(v_N t) \right] \\ &= -i \frac{1}{g} \frac{\pi}{2} \chi_{\eta,\eta'}(t) \operatorname{sgn}(t), \end{aligned} \quad (\text{B9})$$

where we used

$$\ln(it) = \ln(i \operatorname{sgn}(t)) + \ln|t| = \ln|t| + i \frac{\pi}{2} \operatorname{sgn}(t) \quad (\text{B10})$$

and $\lim_{v_N \rightarrow 0^+} \operatorname{sgn}(v_N t) = \operatorname{sgn}(t)$. Also it is quite clear from the derivation that $G_{\eta,\eta'}(x,t) = G_{\eta',\eta}(-x,-t)$.

APPENDIX C: MULTIPLE VERTEX FUNCTION CORRELATOR

Consider the vertex operators $V(q, \vec{r}) = e^{iq\phi(\vec{r})}$. Here we calculate the correlation function of N vertex operators $\langle V(q_1, \vec{r}_1) \cdots V(q_N, \vec{r}_N) \rangle$ with respect to the free boson Lagrangian (A1)

$$\langle V(q_1, \vec{r}_1) \cdots V(q_N, \vec{r}_N) \rangle \equiv \frac{\int \mathcal{D}\phi e^{iS_0[\phi]} e^{i \sum_{j=1}^N q_j \phi(\vec{r}_j)}}{\int \mathcal{D}\phi e^{-S_0[\phi]}}. \quad (\text{C1})$$

Clearly this correlator will have the symmetry Eq. (A2) only when

$$\sum_{j=1}^N q_j = 0 \quad (\text{C2})$$

which is a charge neutrality condition whose important consequence will be shown below. Introducing a source term

$$a(\vec{r}) = \sum_{j=1}^N q_j \delta^{(2)}(\vec{r} - \vec{r}_j), \quad (\text{C3})$$

one can calculate the correlator using path integral as follows:

$$\begin{aligned} \langle V(q_1, \vec{r}_1) \cdots V(q_N, \vec{r}_N) \rangle &= \frac{\int \mathcal{D}\phi e^{iS_0[\phi]} e^{i \int d^2 r a(r) \phi(r)}}{\int \mathcal{D}\phi e^{iS_0[\phi]}} \\ &= e^{-(1/2) \int d^2 r \int d^2 r' a(\vec{r}) G(\vec{r} - \vec{r}') a(\vec{r}')} \\ &= e^{-(1/2) \sum_{j,k=1}^N q_j q_k G(\vec{r}_j - \vec{r}_k)}. \end{aligned} \quad (\text{C4})$$

However, the exponent can be separated into two parts since

$$\begin{aligned} \sum_{j,k=1}^N q_j q_k G(\vec{r}_j - \vec{r}_k) &= \sum_{j,k=1}^N q_j q_k [G(\vec{r}_j - \vec{r}_k) - G(0) + G(0)] \\ &= \left(\sum_{j=1}^N q_j \right)^2 G(0) + \sum_{j,k=1}^N q_j q_k \\ &\quad \times [G(\vec{r}_j - \vec{r}_k) - G(0)] \\ &= \left(\sum_{j=1}^N q_j \right)^2 G(0) + 2 \sum_{j>k=1}^N q_j q_k \\ &\quad \times [G(\vec{r}_j - \vec{r}_k) - G(0)]. \end{aligned} \quad (\text{C5})$$

Notice though $G(0)$ has IR divergence, as it was pointed out in Appendix A, combined with the charge neutrality condition (C2) the correlation function becomes

$$\langle V(q_1, \vec{r}_1) \cdots V(q_N, \vec{r}_N) \rangle = e^{-\sum_{k=1}^N q_j q_k \tilde{G}(\vec{r}_j - \vec{r}_k)}, \quad (\text{C6})$$

where the finite subtracted boson propagator $\tilde{G}(\vec{r}) \equiv G(\vec{r}) - G(0)$ naturally shows up.

APPENDIX D: UNITARY KLEIN FACTORS

Here we derive the unitary Klein factor algebra²³ used in Sec. III and their contour ordering. Anyonic exchange statistics between QP's of different edges l and m defined in Eq. (3.4) requires

$$\psi_l^\dagger \psi_m^\dagger = e^{\pm i\theta} \psi_m^\dagger \psi_l^\dagger. \quad (\text{D1})$$

However, since boson fields commute between different edges, the statistical phase should come solely from the Klein factor algebra. Hence if we define real parameters α_{lm} by

$$F_l F_m = e^{-i\alpha_{lm}} F_m F_l, \quad (\text{D2})$$

the magnitude of α_{lm} follows immediately from comparing Eq. (D1) with the equation

$$\psi_l^\dagger \psi_m^\dagger = e^{-i\alpha_{lm}} \psi_m^\dagger \psi_l^\dagger \quad (\text{D3})$$

to be

$$\alpha_{lm} = \pm \theta = -\alpha_{ml} \quad (\text{D4})$$

leaving the sign of α_{lm} still arbitrary. To consistently fix the correct sign, one must compare the system which is equivalent to Fig. 10(a) with the same topology but where edges are connected with an open contour that brings all the edges into one as in Fig. 10(b) following Guyon *et al.*²³ Klein factors are not necessary in the latter system because the commutation relations of tunneling operators are enforced by the single chiral bosonic field ϕ .

One way of determining Klein factors for case (a) is to compare the relative phases $e^{-i\alpha_{lm}}$ of Fig. 10(a) with the phases $e^{i\theta \operatorname{sgn}(X_l - X_m)}$ of Fig. 10(b) where X_l and X_m are now abscissas of the same edge measured from the point $x=0$ (see the caption of Fig. 10). Another way is to look at the commutation relations of different tunneling operators \hat{V}_l and to

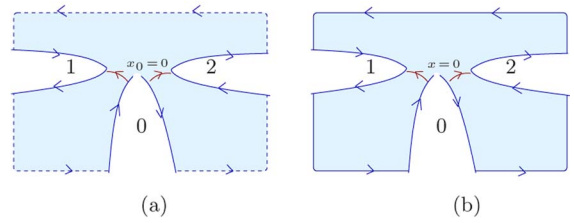


FIG. 10. (Color online) Two configurations with the same topology. (a) Three edges are disconnected and each are described by φ_l with $l=0, 1, 2$. The tunneling to edges $l=1, 2$ occurs at $(x_0=-a/2 \equiv X_1, x_1=0)$ and $(x_0=a/2 \equiv X_2, x_2=0)$, respectively. (b) All three edges are connected with an open contour starting at $x=0$ which is described by a single chiral boson φ . For the tunneling processes to edges $l=1, 2$, QP's hop out from $x=-a/2 \equiv X_1$ and $x=a/2 \equiv X_2$, respectively. We note in passing that since the choice of the origin is arbitrary and do not affect the end result, we made a convenient choice.

require that the commutator of the tunneling operators of the disconnected system give the same results as the connected one.

These two approaches give the same results for the Klein factors and we will choose to detail the second approach here. For the connected system of Fig. 10(b), there is no need for the Klein factors since the tunneling operators at different positions will commute due to chirality (as long as the tunneling paths do not cross). Hence we will set the constraint for α 's by requiring \hat{V}_1 and \hat{V}_2 in the case of interest Fig. 10(a) to commute. First, by comparing the exchange of $\psi(x)\psi(x')$ with that of $\psi^\dagger(x)\psi(x')$ using the CBH formula, one finds that the definition of Eq. (D2) implies

$$F_l F_m^{-1} = e^{i\alpha_{lm}} F_m^{-1} F_l. \quad (\text{D5})$$

With Eqs. (D2) and (D5) we can exchange \hat{V}_1 and \hat{V}_2 at equal time as.

$$\begin{aligned} \hat{V}_1 \hat{V}_2 &= F_0 F_1^{-1} F_0 F_2^{-1} e^{i\varphi_0(x_0=X_1)} e^{i\varphi_0(x_0=X_2)} e^{-i\varphi_1(x_1=0)} e^{-i\varphi_2(x_2=0)} \\ &= F_0 F_2^{-1} F_0 F_2^{-1} e^{i(\alpha_{02}+\alpha_{10}+\alpha_{21})} e^{i\theta \operatorname{sgn}(X_1-X_2)} e^{i\varphi_0(X_2)} e^{i\varphi_0(X_1)} \\ &\quad \times e^{-i\varphi_2(0)} e^{-i\varphi_1(0)} \\ &= e^{i(\alpha_{02}+\alpha_{21}+\alpha_{10})} e^{i\theta \operatorname{sgn}(X_1-X_2)} \hat{V}_2 \hat{V}_1, \end{aligned} \quad (\text{D6})$$

where we used the fact that $[\varphi_l, \varphi_m]=0$ for $l \neq m$ and

$$e^{i\varphi_0(x_0=X_1)} e^{i\varphi_0(x_0=X_2)} = e^{i\theta \operatorname{sgn}(X_1-X_2)} e^{i\varphi_0(X_2)} e^{i\varphi_0(X_1)}. \quad (\text{D7})$$

The second equality followed from QP exchange within edge 0 given by Eq. (2.6) and series of Klein factor exchange as

$$\begin{aligned} F_0 F_1^{-1} F_0 F_2^{-1} &= F_0 F_1^{-1} F_2^{-1} F_0 e^{i\alpha_{02}} = F_0 F_2^{-1} F_1^{-1} F_0 e^{i\alpha_{02}-i\alpha_{12}} \\ &= F_0 F_2^{-1} F_0 F_1^{-1} e^{i\alpha_{02}-i\alpha_{12}+i\alpha_{10}} \\ &= F_0 F_2^{-1} F_0 F_1^{-1} e^{i(\alpha_{02}+\alpha_{21}+\alpha_{10})}. \end{aligned} \quad (\text{D8})$$

From Eq. (D6), requiring \hat{V}_1 and \hat{V}_2 to commute as they would in a single connected edge, results in the constraint

$$\alpha_{02} + \alpha_{21} + \alpha_{10} + \theta \operatorname{sgn}(X_1 - X_2) = 0, \quad (\text{D9})$$

which allows us to define $\alpha_{02} = \alpha_{21} = -\alpha_{10} = \theta$ since $X_2 - X_1 = a > 0$ (see the caption of Fig. 10). Further we can conclude

$$F_0 F_1^{-1} F_0 F_2^{-1} = F_0 F_2^{-1} F_0 F_1^{-1} e^{i\theta}. \quad (\text{D10})$$

Now we determine the contour ordered Klein factor “propagator” $\langle T_K(F_0 F_1^{-1})^\epsilon(t^\eta)(F_0 F_2^{-1})^{\epsilon'}(t'^{\eta'}) \rangle_0$ based on Eq. (D10). We first note contour ordering means that $(F_0 F_1^{-1})^\epsilon(t^\eta)$ and $(F_0 F_2^{-1})^{\epsilon'}(t'^{\eta'})$ need to be exchanged whenever $t'^{\eta'} > K t^\eta$, i.e.,

$$\begin{aligned} & \langle T_K(F_0 F_1^{-1})^\epsilon(t^\eta)(F_0 F_2^{-1})^{\epsilon'}(t'^{\eta'}) \rangle_0 \\ &= \begin{cases} \langle (F_0 F_1^{-1})^\epsilon(t^\eta)(F_0 F_2^{-1})^{\epsilon'}(t'^{\eta'}) \rangle & \text{for } t'^{\eta'} > K t^\eta, \\ \langle (F_0 F_2^{-1})^{\epsilon'}(t'^{\eta'})(F_0 F_1^{-1})^\epsilon(t^\eta) \rangle & \text{for } t'^{\eta'} < K t^\eta. \end{cases} \end{aligned} \quad (\text{D11})$$

From Eq. (D10), it is clear that a consistent way of defining the contour ordered propagator is to assign a relative phase factor of $e^{-i\theta \operatorname{sgn}(X_1 - X_2)}$ between $t'^{\eta'} > K t^\eta$

case (in which the Klein factors need to be exchanged for contour ordering) and $t'^{\eta'} < K t^\eta$ case (in which no exchange is necessary). Further in order for $\langle T_K \hat{V}_1(t^\eta) \hat{V}_2(t'^{\eta'}) \rangle = \langle T_K \hat{V}_2(t'^{\eta'}) \hat{V}_1(t^\eta) \rangle$ to hold, which would be the case for the connected edge and which connects us back to the basis for the derivation of Eq. (D10), we require

$$\begin{aligned} & \langle T_K(F_0 F_1^{-1})^\epsilon(t^\eta)(F_0 F_2^{-1})^{\epsilon'}(t'^{\eta'}) \rangle \\ &= \langle T_K(F_0 F_2^{-1})^{\epsilon'}(t'^{\eta'})(F_0 F_1^{-1})^\epsilon(t^\eta) \rangle. \end{aligned} \quad (\text{D12})$$

This last requirement can be satisfied by assigning half of the relative phase factor $e^{-i\theta \operatorname{sgn}(X_1 - X_2)}$ to each case of Eq. (D11) and we arrive at the following form:

$$\begin{aligned} & \langle T_K(F_0 F_1^{-1})^\epsilon(t^\eta)(F_0 F_2^{-1})^{\epsilon'}(t'^{\eta'}) \rangle_0 \\ &= e^{i\epsilon\epsilon'(\theta/2)\operatorname{sgn}(X_1 - X_2)\chi_{\eta,\eta'}(t-t')} = e^{-i\epsilon\epsilon'(\theta/2)\chi_{\eta,\eta'}(t-t')}, \end{aligned} \quad (\text{D13})$$

where we used the definition of $\chi_{\eta,\eta'}(t-t')$ introduced for the contour ordered propagator of chiral bosons in Eq. (B6).

-
- ¹J. Leinaas and J. Myrheim, Nuovo Cimento Soc. Ital. Fis., B **37**, 1 (1977).
²F. Wilczek, Phys. Rev. Lett. **48**, 1144 (1982).
³D. C. Tsui, H. L. Störmer, and A. C. Gossard, Phys. Rev. Lett. **48**, 1559 (1982).
⁴R. B. Laughlin, Phys. Rev. Lett. **50**, 1395 (1983).
⁵D. Arovas, J. R. Schrieffer, and F. Wilczek, Phys. Rev. Lett. **53**, 722 (1984).
⁶B. I. Halperin, Phys. Rev. Lett. **52**, 1583 (1984).
⁷F. D. M. Haldane, Phys. Rev. Lett. **67**, 937 (1991).
⁸R. A. J. van Elburg and K. Schoutens, Phys. Rev. B **58**, 15704 (1998).
⁹X. G. Wen and Q. Niu, Phys. Rev. B **41**, 9377 (1990).
¹⁰X. G. Wen, Am. J. Optom. Physiol. Opt. **44**, 405 (1995).
¹¹V. J. Goldman and B. Su, Science **267**, 1010 (1995).
¹²R. de Picciotto, M. Reznikov, M. Heiblum, V. Umansky, G. Bunin, and D. Mahalu, Nature (London) **389**, 162 (1997).
¹³L. Saminadayar, D. C. Glattli, Y. Jin, and B. Etienne, Phys. Rev. Lett. **79**, 2526 (1997).
¹⁴M. Reznikov, R. de Picciotto, T. G. Griffiths, M. Heiblum, and V. Umansky, Nature (London) **399**, 238 (1999).
¹⁵J. K. Jain, Phys. Rev. Lett. **63**, 199 (1989).
¹⁶R. Hanbury-Brown and Q. R. Twiss, Nature (London) **177**, 27 (1956).
¹⁷A. López and E. Fradkin, Phys. Rev. B **59**, 15323 (1999).
¹⁸E.-A. Kim, M. Lawler, S. Vishveshwara, and E. Fradkin, Phys. Rev. Lett. **95**, 176402 (2005).
¹⁹X. G. Wen, Phys. Rev. B **41**, 12838 (1990).
²⁰A. López and E. Fradkin, Phys. Rev. B **44**, 5246 (1991).
²¹A. Chang, Rev. Mod. Phys. **75**, 1449 (2003).
²²I. Safi, P. Devillard, and T. Martin, Phys. Rev. Lett. **86**, 4628 (2001).
²³R. Guyon, P. Devillard, T. Martin, and I. Safi, Phys. Rev. B **65**, 153304 (2002).
²⁴C. de C. Chamon, D. E. Freed, and X. G. Wen, Phys. Rev. B **51**, 2363 (1995).
²⁵C. de C. Chamon, D. E. Freed, and X. G. Wen, Phys. Rev. B **53**, 4033 (1996).
²⁶L. V. Keldysh, Zh. Eksp. Teor. Fiz. **47**, 1515 (1964) [Sov. Phys. JETP **20**, 1018 (1965)].
²⁷L. P. Kadanoff and G. Baym, *Quantum Statistical Mechanics* (Benjamin, New York, 1962).
²⁸J. Rammer and H. Smith, Rev. Mod. Phys. **58**, 323 (1986).
²⁹S. Vishveshwara, Phys. Rev. Lett. **91**, 196803 (2003).
³⁰S. C. Zhang, T. H. Hansson, and S. Kivelson, Phys. Rev. Lett. **62**, 82 (1989).
³¹C. L. Kane and M. P. A. Fisher, Phys. Rev. Lett. **68**, 1220 (1992); **72**, 724 (1994).
³²J. K. Jain, S. A. Kivelson, and D. J. Thouless, Phys. Rev. Lett. **71**, 3003 (1993).
³³C. de C. Chamon, D. E. Freed, S. A. Kivelson, S. L. Sondhi, and X. G. Wen, Phys. Rev. B **55**, 2331 (1997).
³⁴C. L. Kane, Phys. Rev. Lett. **90**, 226802 (2003).
³⁵K. T. Law, D. E. Feldman, and Y. Gefen Phys. Rev. B **74**, 045319 (2006).
³⁶F. E. Camino, W. Zhou, and V. J. Goldman, Phys. Rev. Lett. **95**, 246802 (2005).
³⁷F. E. Camino, W. Zhou, and V. J. Goldman, cond-mat/0510764 (unpublished).
³⁸W. Zhou, F. E. Camino, and V. J. Goldman, cond-mat/01512329 (unpublished).
³⁹E. Fradkin, C. Nayak, A. Tsvelik, and F. Wilczek, Nucl. Phys. B **516**, 704 (1998).
⁴⁰S. Das Sarma, M. Freedman, and C. Nayak, Phys. Rev. Lett. **94**,

- 166802 (2005).
⁴¹F. D. M. Haldane, Phys. Rev. Lett. **51**, 605 (1983).
⁴²E.-A. Kim, cond-mat/0604359 (unpublished).
⁴³Y. C. Chung, M. Heiblum, and V. Umansky, Phys. Rev. Lett. **91**, 216804 (2003).
⁴⁴A. Y. Kitaev, Ann. Phys. (N.Y.) **303**, 2 (2003).
⁴⁵D. H. Lee and X. G. Wen, cond-mat/9809160 (unpublished).